Tumor-Associated Fibroblasts Promote HER2-Targeted Therapy Resistance through FGFR2 Activation

Patricia Fernández-Nogueira[1,2], Mario Mancino[1,2], Gemma Fuster[1], Anna López-Plana[1], Patricia Jauregui[1], Vanesa Almendro[3], Estel Enreig[1,2], Silvia Menéndez[4], Federico Rojo[5], Aleix Noguera-Castells[1,2], Anke Bill[6], L. Alex Gaither[6], Laia Serrano[4], Leire Recalde-Percaz[1,2], Núria Moragas[1,2], Raul Alonso[1], Elisabet Ametller[1], Ana Rovira[7,8], Ana Lluch[9,10], Joan Albanell[7,8,11], Pere Gascon[1,2,12], and Paloma Bragado[1,13]

ABSTRACT

Purpose: Despite the therapeutic success of existing HER2-targeted therapies, tumors invariably relapse. This study aimed at identifying new mechanisms responsible for HER2-targeted therapy resistance.

Experimental Design: We have used a platform of HER2-targeted therapy–resistant cell lines and primary cultures of healthy and tumor-associated fibroblasts (TAF) to identify new potential targets related to tumor escape from anti-HER2 therapies.

Results: We have shown that TAFs promote resistance to HER2-targeted therapies. TAFs produce and secrete high levels of FGF5, which induces FGFR2 activation in the surrounding breast cancer cells. FGFR2 transactivates HER2 via c-Src, leading to resistance to HER2-targeted therapies. *In vivo*, coinoculating nonresistant cell lines with TAFs results in more aggressive and resistant tumors. Resistant cells activate fibroblasts and secrete FGFR ligands, creating a positive feedback loop that fuels resistance. FGFR2 inhibition not only inhibits HER2 activation, but also induces apoptosis in cells resistant to HER2-targeted therapies. *In vivo*, inhibitors of FGFR2 reverse resistance and resensitize resistant cells to HER2-targeted therapies. In HER2 patients' samples, α-SMA, FGF5, and FGFR2 contribute to poor outcome and correlate with c-Src activation. Importantly, expression of FGF5 and phospho-HER2 correlated with a reduced pathologic complete response rate in patients with HER2-positive breast cancer treated with neoadjuvant trastuzumab, which highlights the significant role of TAFs/FGF5 in HER2 breast cancer progression and resistance.

Conclusions: We have identified the TAF/FGF5/FGFR2/c-Src/HER2 axis as an escape pathway responsible for HER2-targeted therapy resistance in breast cancer, which can be reversed by FGFR inhibitors.

Introduction

Breast cancer, the most common malignancy and the leading cause of cancer-related death among women worldwide (1), is a very heterogeneous disease. In the past 15 years, gene expression profiling has identified and characterized 5 intrinsic molecular subtypes of breast cancer (Luminal A, Luminal B, HER2 enriched, basal-like and Claudin-low) associated with distinct clinical outcomes (2–4). HER2-positive tumors account for 15% to 20% of all breast malignancies and have an aggressive clinical course (5). Pertuzumab, trastuzumab, and lapatinib are the most commonly used drugs targeting HER2, and they have demonstrated excellent therapeutic effects (6). However, the development of resistance to these treatments has dampened their success (7–9).

The mechanisms by which cancer cells acquire resistance to drugs involve not only cell-autonomous processes such as genetic and epigenetic alterations, but also the tumor microenvironment (10). The tumor stromal compartment consists of an extracellular matrix and different types of cells, including tumor-associated fibroblasts (TAF), immune and inflammatory cells, endothelial cells, and adipocytes, among others (11). Cancer cells are in constant communication with the cells in the tumor microenvironment, and stromal cells are actively recruited into the tumor. Furthermore, cancer cells release stroma-modulating factors, such as fibroblast growth factors, that act in a paracrine manner, disrupting normal tissue homeostasis and modifying the stroma to provide cancer cells with a supportive microenvironment for tumor progression (12).

Under normal physiologic conditions, fibroblasts serve as an important barrier to epithelial cell transformation and inhibit tumor growth (13). However, TAFs in mammary carcinomas are very different from fibroblasts from healthy stroma in several important functional aspects (14). TAFs are cells with an activated phenotype, identifiable by the expression of α-smooth muscle actin (α-SMA) among other markers, that produce growth factors and extracellular matrix proteins that promote proliferation and survival of tumor

[1]Molecular and Translational Oncology Group, Institut d'Investigacions Biomediques August Pi i Sunyer (IDIBAPS), Barcelona, Spain. [2]Department of Medicine, University of Barcelona, Barcelona, Spain. [3]Division of Medical Oncology, Department of Medicine, Harvard Medical School, Dana-Farber Cancer Institute, Brigham and Women's Hospital, Boston, Massachusetts. [4]Pathology Department, Hospital del Mar, Barcelona, Spain. [5]Pathology Department, CIBERONC-IIS-Fundación Jiménez Díaz, Madrid, Spain. [6]Novartis Institutes for BioMedical Research, Inc., Cambridge, Massachusetts. [7]Cancer Research Program, IMIM (Hospital del Mar Research Institute), Barcelona, Spain. [8]Medical Oncology Department, Hospital del Mar-CIBERONC, Barcelona, Spain. [9]INCLIVA Biomedical Research Institute, Universitat de València, Valencia, Spain. [10]Oncology and Hematology Department, CIBERONC-Hospital Clínico Universitario, Valencia, Spain. [11]Universitat Pompeu Fabra, Barcelona, Spain. [12]Department of Medical Oncology, Hospital Clínic, Barcelona, Spain. [13]Department of Biochemistry and Molecular Biology, Faculty of Pharmacy, Complutense University of Madrid, Health Research Institute of the Hospital Clínico San Carlos, Madrid, Spain.

Note: Supplementary data for this article are available at Clinical Cancer Research Online (http://clincancerres.aacrjournals.org/).

P. Gascon and P. Bragado have contributed equally to this article.

Corresponding Authors: Paloma Bragado, Department of Biochemistry and Molecular Biology, Faculty of Pharmacy, Complutense University of Madrid, Plaza de Ramon y Cajal, s/n, 28040, Madrid, Spain. Phone: 34913941853; E-mail: pbragado@ucm.es; and Pere Gascón, Institut d'Investigacions Biomédiques August Pi i Sunyer (IDIBAPS), Carrer de Rosello 149-153, Barcelona 08036, Spain. Phone: 34932275400-4301; E-mail: gascon@clinic.cat

Clin Cancer Res 2020;26:1432–48

doi: 10.1158/1078-0432.CCR-19-0353

Translational Relevance

Although the development of HER2-targeted therapies has changed the course of treatment in patients with HER2-positive breast cancer, tumors invariably relapse. Here, we show that tumor-associated fibroblast secretion of FGF5 promotes HER2-targeted therapy resistance by inducing fibroblast growth factor receptor 2 (FGFR2) activation in breast cancer cells. FGFR2 transactivates HER2 through c-Src promoting survival. We have demonstrated that inactivating FGFR2 reduces HER2 activity and sensitizes resistant cells to trastuzumab and lapatinib, overcoming HER2-targeted therapy resistance. Furthermore, in HER2-positive patients, overexpression of α-SMA, FGF5, FGFR2, and phospho-HER2 correlated with phospho-c-Src expression and worse prognosis. Finally, combined elevated expression of FGF5 and phospho-HER2 correlated with lack of pathologic complete response and worse disease-free survival in patients treated with trastuzumab-based neoadjuvant therapy. Therefore, we have identified a clinically relevant approach for HER2 breast cancer therapy that can be exploited to delay the onset of resistance.

cells (15). Increased numbers of TAFs in the stroma of different human cancers are associated with increased risk of invasion, metastasis, and poor clinical prognosis (16).

Increasing evidence suggests that TAFs play an important role in resistance to endocrine therapy, chemotherapy, and targeted therapies (17). In addition, Howell and colleagues found that increased expression of a specific stromal gene signature was a strong negative predictive factor for response to neoadjuvant chemotherapy in patients with ER-negative breast cancer, thus supporting the concept that targeting the microenvironment can improve clinical response in these patients (18). At least 80% of stromal fibroblasts in breast cancer are thought to have an activated phenotype (19). Because TAFs are considerably more genetically homogeneous than cancer cells, they are less likely to acquire resistance to drugs, making them an attractive target for cancer therapy (20).

Cell-autonomous resistance to anti-HER2 therapies can develop through various mechanisms, including *PI3K* or *PTEN* mutations (21), overexpression of the transmembrane receptor MUC4 that allosterically affects the interaction between the antibody and the receptor, poor immune system recognition (22), and cross-talk with other tyrosine kinase receptors such as HER3 (23) or insulin growth factor receptor (IGF-R1; ref. 24). However, the role of fibroblasts in the acquisition of resistance to trastuzumab and lapatinib in HER2-positive breast cancer has not been widely explored. Therefore, we have used fibroblasts isolated from healthy donors and from patients with breast cancer to study the cross-talk between fibroblasts and breast cancer cells. We have also developed a platform to identify new targets related to tumor escape from anti-HER2 therapies.

Materials and Methods

Cell lines and cultures

Human breast cancer cell lines (MDA-MB-453, BT-474, and SK-BR-3) were obtained from the ATCC (2008–2009) and validated by single locus short tandem repeat typing (Bio-Synthesis, Inc.) before its use. Cells were cultured under a humidified atmosphere of 5% CO_2 at 37°C in DMEM-F12 (Gibco) growing medium, supplemented with 10% FBS (Gibco), 5% Glutamax (Gibco), and 5% fungizone–penicillin–streptomycin mixture (Invitrogen), hereafter referred to as complete culture medium. For the BT-474 cell line, 10 μg/mL of insulin (Sigma) was added to the media. *Mycoplasma* test (EZ-PCR Mycoplasma Test Kit, Biological Industries) was performed every two weeks to ensure culture conditions.

All cell lines were infected with a lentiviral pBabe-Puro construct encoding a puromycin-resistant gene and also expressing mCherry-LUC, using X-treme GENE 9 reagent (Roche), at a 1:6 ratio (DNA: transfection reagent). After infection, cells were cultured in the presence of puromycin to select the cells that had incorporated the vector, and finally mCherry-LUC–positive cells were sorted by flow cytometry.

Generation of mCherry-LUC$^+$ breast cancer cell lines resistant to trastuzumab and lapatinib

MDA-MB-453, BT-474, and SK-BR-3 cell lines were initially grown in media containing 1 μmol/L of lapatinib and 100 μg/mL of trastuzumab. The concentration was gradually increased over the following 5 months to 4 μmol/L of lapatinib and 200 μg/mL of trastuzumab to establish lapatinib-resistant (SK-BR-3-LAP, BT-474-LAP, MDA-MB-453-LAP) and trastuzumab-resistant (SK-BR-3-TZ, BT-474-TZ, MDA-MB-453-TZ) cell lines (Supplementary Fig. S1A).

Generation of human-derived fibroblast cell lines

To establish the nontumor-associated fibroblast cell lines, we obtained fresh healthy mammary tissue from women undergoing reduction mammoplasty. To establish the TAF cell lines, a tumorectomy specimen was collected from 4 patients with breast cancer (two HER2^{+++} patients, and two HER2$^-$ patients). All samples were collected under the approval of the Institutional Review Board of Clinica Planas and Hospital Clinic in Barcelona, informed consent was obtained from all subjects. Tissue from all specimens was minced into small pieces and digested to further isolate the fibroblast population. Fibroblasts were seeded in 10% FBS-DMEM medium and placed in a plastic plate to be cultured in regular conditions (37°C in a humidified 5% CO_2 atmosphere). To select the fibroblasts and separate them from all the other cell populations in the sample, we applied differential trypsinization.

To immortalize the primary human normal mammary fibroblasts from reduction mammoplasties (RMF) and TAFs, a retroviral vector pMIG (MSCV-IRES-GFP; kindly provided by Kornelia Polyak, Dana-Farber Cancer Institute, Brigham and Women's Hospital, Boston, Massachusetts) expressing both hTERT and GFP was introduced, using X-tremeGENE transfection reaction (Roche), at a 1:6 ratio (DNA: transfection reagent). Fibroblasts were cultured for 4 to 5 days and then the GFP$^+$ cells were sorted using flow cytometry (Supplementary Fig. S1B).

Conditioned media experiments

For the experiments with conditioned media, cells were plated in 150 cm^3 until subconfluence; fresh complete culture medium was added, and cells were incubated with 15 mL of medium for 72 hours. The supernatant was recovered, filtered, and centrifuged (1,200 rpm for 5 minutes) to discard unattached cells and cell debris.

Cell viability studies

To determine cell proliferation in parental and drug-resistant cell lines, the Cell Titer 96 Aqueous One Solution Cell Proliferation Assay Kit (Promega) was used following the manufacturer's instructions. Briefly, subconfluent cultures of the different cell lines were incubated

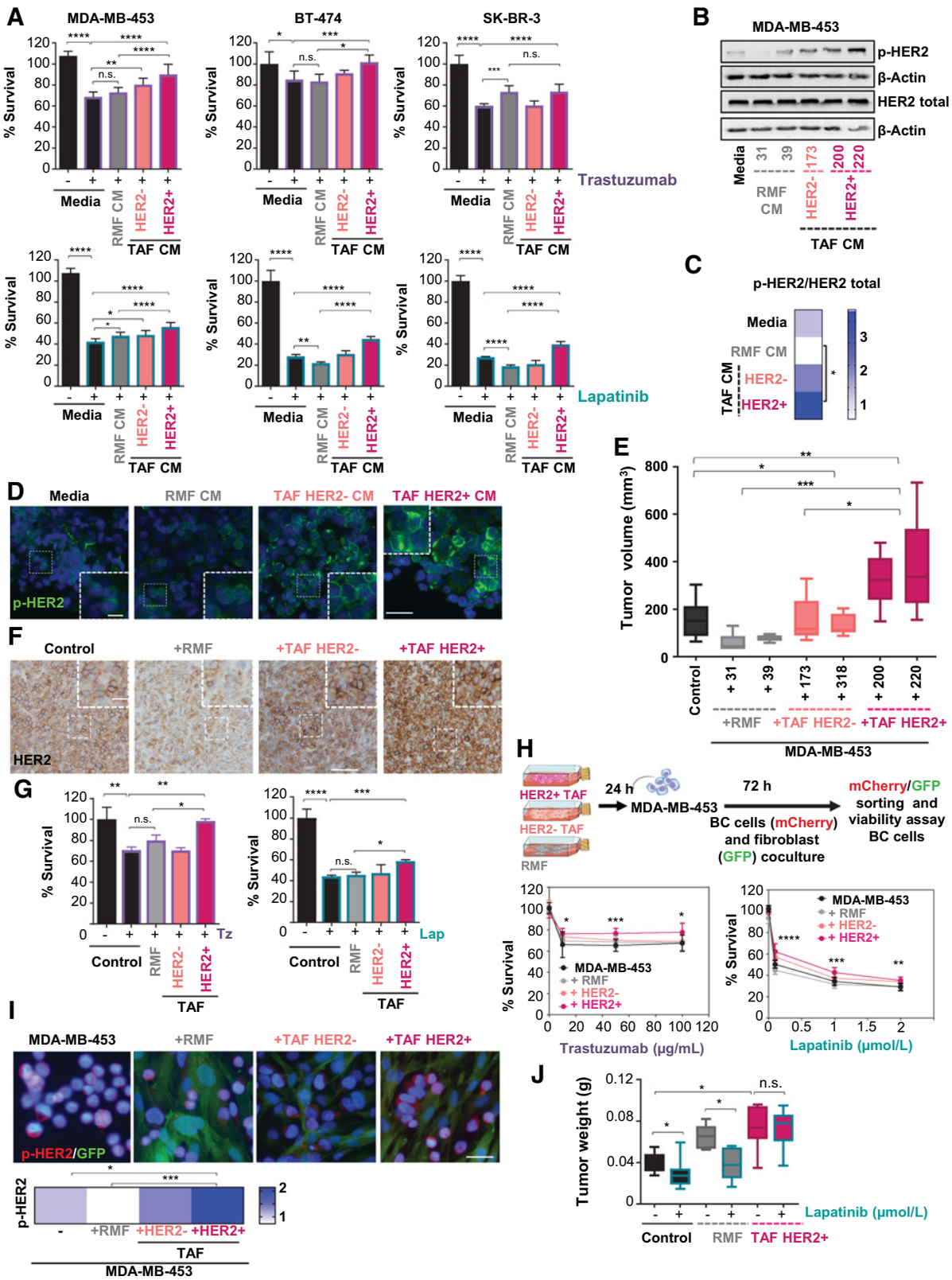

for 72 hours in the presence of lapatinib (0–5 μmol/L) or trastuzumab (0–250 μg/mL) in 96-well plates. For lapatinib assays, the corresponding dose of DMSO used as drug solvent (never above 0.02% v/v) was added to the control wells as dose 0.

Experiments in mice

All animal experiments were performed in accordance with our institution's ethics commission's regulations, following the guidelines established by the regional authorities (Catalonia, Spain). The mice (5-week-old female CB17/Icr Hand-PrKdcscid or 5-week-old female athymic nude Foxn 1nu nu/nu) were bred at the medical school's animal facility laboratory and kept under specific pathogen-free (SPF) conditions at constant ambient temperature (22°C–24°C) and humidity (30%–50%). The mice had access to sterilized food and tap water *ad libitum*. After each experiment, the animals were anesthetized and euthanized in accordance with our institution's ethics commission's regulations. Details of specific animal experiments are fully described in Supplementary Materials and Methods.

In vivo chicken embryo model

For the chorioallantoic membrane (CAM) xenografts, we used premium SPF, fertile, 11-day–incubated embryonated chicken eggs. We coinoculated 1×10^6 MDA-MB-453 cells, alone or together with fibroblasts from different origins (RMF-39, TAF-220; ratio 1:1, diluted in PBS and Matrigel) and tumors were grown for 6 days. The day after inoculation, the tumors were treated with lapatinib 1 μmol/L daily for 5 days. On day 6 after inoculation, the tumors were excised, weight, and measured.

Annexin V staining

Apoptosis was determined using Annexin-V-FLUOS Staining Kit (Biovision) according to the manufacturer's instructions. Briefly, cells from the culture supernatants and those attached to the plate were blocked for 30 minutes with 1% BSA and then incubated for 15 minutes at 4°C with Annexin V-FITC solution and propidium iodide (PI). Controls (binding buffer only, PI only, and Annexin-V only) were used to set appropriate detector gains, compensation, and quadrant gates in the FACSCalibur flow cytometer. A total of 20,000 cells for each sample were analyzed with the Cell Quest software.

Activated HER2 FACS

SK-BR-3, MDA-MB-453, and BT-474 parental and resistant cells lines were detached with PBS-EDTA 2 mmol/L, washed, and pre-incubated for 20 minutes with cold PBS + 1% BSA. Then, the cells were incubated with the primary antibody against activated HER2 (Y1248; Millipore) at 1:60 dilution at 4°C for 1 hour. The antibody was conjugated with an Alexa Fluor 488. Cells were then washed twice and incubated with PI for 15 minutes. Finally, cells were washed twice and suspended in sorting buffer (EDTA 1 mmol/L, HEPES 25 mmol/L, and BSA 1%). The cells were analyzed using a BD Biosciences FACSAria III cell sorter.

FGF2 and FGF5 ELISA

FGF2 and FGF5 levels were determined using a quantitative solid-phase sandwich ELISA (FGF2 Thermo Fisher Scientific and FGF5 LifeSpan, Inc.) and tested in triplicate following the manufacturer's instructions. Test sensitivity ranged from 15.6 to 1,000 pg/mL for FGF2 and 24.58 to 6,000 pg/mL for FGF5. Levels were determined using the standard sigmoidal curve to find the corresponding concentration calculated with the GraphPad software.

Patient studies

Breast tissues were surgical resection specimens from primary tumors from consecutive breast cancers patients diagnosed between 1998 and 2000. The study was approved by the Ethics Committees of each of the three hospitals involved in the study through cooperative research and conducted following institutional guidelines. All experiments conformed to the principles set out in the WMA Declaration of Helsinki and the Department of Health and Human Services Belmont

Figure 1.

Cross-talk between TAFs and breast cancer cells promotes a more aggressive phenotype and cell resistance to anti-HER2 therapies. **A,** Cell survival after treatment for 48 hours with trastuzumab (100 μg/mL) or lapatinib (2 μmol/L) in cells treated with normal media (media) or conditioned media from healthy stroma fibroblasts (RMF), HER2-negative TAFs (HER2$^-$ TAF) or HER2-positive TAFs (HER2$^+$ TAF). The graphs show the percentage of survival. Data, mean ± SD; $n = 3$. **B,** Representative Western blot analysis of phospho-HER2 (Y1221/1222), total HER2, and β-actin in parental MDA-MB-453 cell lines treated for 24 hours with normal media (media) or conditioned media from healthy stroma fibroblasts (RMF CM), HER2-negative TAFs (HER2$^-$ TAF CM) or HER2-positive TAFs (HER2$^+$ TAF CM). The β-actin controls in **Figs. 1B** and **2I** are the same because it is the same experiment and the antibodies were done in the same membrane. **C,** Heatmap depicting densitometric quantification of the Western blot analyses in **B**, expressed as the ratio of activated versus total HER2 expression relative to the expression of β-actin. Data, mean ± SD; $n = 3$. **D,** Representative images of activated HER2 staining (Y1248, phosphorylated levels represented as p-, in green) in parental MDA-MB-453 cells cultured with normal media (media) or fibroblast-derived conditioned media (CM) for 72 hours. RMF (RMF-31), TAF HER2$^-$ (TAF-173), and TAF HER2+ (TAF-200). Scale bar, 100 μm. Magnification scale bar, 50 μm. **E,** Tumor volume 90 days after orthotopic coinoculation in the mammary gland of MDA-MB-453 cells alone (control) or with the different fibroblast cell lines: healthy stroma fibroblasts (RMF31, RMF39), HER2-negative TAFs (TAF HER2$^-$ 173 and 318) or HER2-positive TAFs (TAF HER2$^+$ 200 and 220). Data, mean ± SD; $n = 5$. **F,** Representative images showing HER2 staining in tumors of MDA-MB-453 cells coinjected alone (control) or with the different fibroblast cell lines: healthy stroma fibroblasts (+ RMF), HER2-negative TAFs (+ TAF HER2$^-$), or HER2-positive TAFs (+ TAF HER2$^+$). Scale bar, 50 μm. Magnification scale bar, 25 μm. **G,** Quantification of cell viability represented as percentage of survival in MDA-MB-453 mCherry$^+$ cells isolated from tumors derived from the orthotopic coinoculation of MDA-MB-453 alone (control) or with the different fibroblast cell lines [healthy stroma fibroblasts (RMF), HER2-negative TAFs (HER2$^-$ TAF) or HER2-positive TAFs (HER2$^+$ TAF); **E**)], treated for 72 hours with trastuzumab (100 μg/mL) and lapatinib (4 μmol/L). Data, mean ± SD; $n = 3$. **H,** Diagram representing MDA-MB-453 72-hour coculture with fibroblasts from different origin [healthy stroma fibroblasts (RMF), HER2-negative TAFs (HER2$^-$ TAF), or HER2-positive TAFs (HER2$^+$ TAF)] and consecutive cell sorting of the mCherry$^+$ population of BC cells. Graphs below show quantification of cell viability, represented as percentage of survival of the sorted cells treated with increasing doses of trastuzumab (0–100 μg/mL) and lapatinib (0–2 μmol/L) for 48 hours. Black lines represent MDA-MB-453 cells cultured alone; gray lines represent MDA-MB-453 cells cultured with healthy stromal fibroblasts (RMF-31); light pink lines represent MDA-MB-453 cells cultured with HER2-negative TAFs (HER2$^-$ TAF-318); dark pink lines represent MDA-MB-453 cells cultured with HER2-positive TAFs (HER2$^+$ TAF-200). Data, mean ± SD, $n = 3$. **I,** Representative images showing activated HER2 levels (Y1248, phosphorylated levels represented as p-, in red) in MDA-MB-453 cells cocultured with GFP$^+$ fibroblast cell lines in green for 72 hours [healthy stroma fibroblasts (RMF31), HER2-negative TAFs (HER2$^-$ TAF-318) or HER2-positive TAFs (HER2$^+$ TAF-200)]. Scale bar, 150 μm. Heatmap below shows activated HER2 levels quantified as mean fluorescence intensity (MFI). Data, mean ± SD; $n = 3$. **J,** Tumor weight 6 days after orthotopic coinoculation in the CAM of day 11 chicken embryos of MDA-MB-453 cells alone (control) or with the different fibroblast cell lines: healthy stroma fibroblasts (RMF39) and HER2-positive TAFs (TAF HER2$^+$ 220) treated daily for 5 days with lapatinib 1 μmol/L. Data, mean ± SD; $n = 5$. n.s., nonsignificant; *, $P < 0.05$; **, $P < 0.01$; ***, $P < 0.001$; ****, $P < 0.0001$ by ANOVA with Sidak *post hoc* multiple comparison test.

Report. Representative areas of each tumor were carefully selected and three tissue cores (1 mm diameter) were obtained using a TMA workstation (T1000 Chemicon). An additional cohort of 64 patients diagnosed of early HER2-positive breast cancer treated with neoadjuvant trastuzumab-containing therapy was selected, and pretreatment diagnostic core biopsies were assayed. Pathologic complete response (pCR) was defined as no histologic evidence of invasive disease both in breast and axillary lymph nodes. For further details about IHC staining and quantification, see human samples and histologic scoring section in Supplementary Materials and Methods section.

Results

Cross-talk between TAFs and breast cancer cells promotes a more aggressive phenotype and cell resistance to anti-HER2 therapies

To examine the potential impact of fibroblasts on resistance to trastuzumab and lapatinib, we developed several fibroblast cell lines from different origins: fibroblasts from healthy breast tissue obtained from reduction mammoplasties [reduction mammoplasties fibroblasts (RMF-31 and RMF-39)], and fibroblasts associated with HER2-negative and HER2-positive breast tumors obtained from tumorectomies in different patients, hereafter referred to as HER2-negative TAFs (TAF-173 and TAF-318) and HER2-positive TAFs (TAF-200 and TAF-220; Supplementary Fig. S1B). Then, we analyzed the fibroblasts' activation profile by measuring their expression of fibroblasts specific protein (FSP), α-SMA and S100 calcium binding protein A4 (S100A4; Supplementary Fig. S1C and S1D). As reported elsewhere (25), the expression of FSP, α-SMA, and S100A4 was higher in TAF cell lines than in healthy fibroblast cell lines (Supplementary Fig. S1C and S1D).

We first tested the effect of fibroblast conditioned media on HER2-positive breast cancer cells proliferation. We cultured the fibroblast cell lines for 48 hours and collected the conditioned media and cultured HER2-positive breast cancer cells in this fibroblast-conditioned media for 72 hours. We found that treatment with either healthy stroma fibroblasts or HER2-negative TAFs or HER2-positive TAFs derived conditioned media did not affect breast cancer cells proliferation *in vitro* (Supplementary Fig. S2A). To determine the contribution of the fibroblast population to resistance to trastuzumab and lapatinib, we treated HER2-positive breast cancer cell lines with trastuzumab and lapatinib in the presence or absence of the fibroblast-conditioned media and performed cell proliferation assays (**Fig. 1A**). Interestingly, exposing cells to TAFs conditioned media promoted survival in all cell lines in the presence of trastuzumab and lapatinib (**Fig. 1A**). Sensitivity to trastuzumab and lapatinib was reduced even more in the cells exposed to the conditioned media from cultures of HER2-positive TAFs (**Fig. 1A**). On the contrary, culturing cells with normal fibroblast conditioned media had little effect, except for the SK-B-R3 cells treated with trastuzumab, or even decreased survival in the presence of lapatinib (**Fig. 1A**). Interestingly, incubation of MDA-MB-453 cells with TAFs cultures conditioned media induced HER2 activation (**Fig. 1B–D**; Supplementary Fig. S2B), which was greater when the cells were exposed to the medium derived from HER2-positive TAFs. These results suggest that TAFs secrete soluble factors that can induced resistance to trastuzumab and lapatinib by maintaining HER2 activated.

To investigate breast cancer cell cross-talk with TAFs *in vivo*, we coinoculated MDA-MB-453 cells, alone or together with fibroblasts from different origins into the mammary fad pads of SCID mice. The tumors growing from the MDA-MB-453 cells injected together with the HER2-positive TAFs grew slightly faster than those growing from MDA-MB-453 cells injected with the other types of fibroblasts or from MDA-MB-453 cells alone; furthermore, coinoculation with HER2-positive TAFs gave rise to larger tumors (**Fig. 1E**), suggesting that these fibroblasts promote tumor proliferation and survival. Interestingly, coinoculation with healthy stroma fibroblasts resulted in smaller and less aggressive tumors, suggesting these nonactivated fibroblasts might play a protective role against tumor growth (**Fig. 1E**). In agreement with our *in vitro* findings, the tumors developing after the coinoculation of MDA-MB-453 cells with HER2-positive TAFs showed higher HER2 expression (**Fig. 1F**), whereas the tumors developing from the coinoculation with healthy stroma fibroblasts showed lower HER2 expression (**Fig. 1F**). When we analyzed the stroma of the tumors, we found that the tumors developing from the coinoculation with HER2-positive TAFs had more α-SMA–positive infiltrating fibroblasts than those developing from inoculation with MDA-MB-453 cells alone or together with HER2-negative TAFs or with healthy stroma fibroblasts (Supplementary Fig. S2C).

To test whether coevolution of breast cancer cells with the fibroblasts changed the phenotype of the MDA-MB-453 cells, we established primary cultures from each tumor and tested their sensitivity to trastuzumab and lapatinib. Proliferation assays showed that the cells from tumors that developed from coinoculation with HER2-positive TAFs had a phenotype that was more resistant to anti-HER2 therapies (**Fig. 1G**). The analysis of HER2 expression in these primary cultures further showed that the HER2 overexpression found in the tumors *in vivo* was maintained over time in the primary cultures derived from these tumors (Supplementary Fig. S2D and E). To determine if the effect that we observed *in vivo* was mediated directly by the fibroblasts and not by other populations recruited to the tumor, we seeded MDA-MB-453-mCherry cells with the different populations of fibroblasts for 72 hours. Then, we sorted MDA-MB-453-mCherry cells to separate them from the fibroblasts (GFP positive) and seeded and treated them with lapatinib or trastuzumab to assess viability (**Fig. 1H**; Supplementary Fig. S2F). We found that coculture with normal fibroblasts did not affect breast cancer cells viability; however, coculture for 72 hours in the presence of TAFs increased viability and induced resistance to both trastuzumab and lapatinib (**Fig. 1H**). As in the previous experiments, this protective effect was more pronounced when the cells were cocultured with HER2-positive TAFs (**Fig. 1H**). Furthermore, our results also showed that coculture with TAFs induced HER2 activation in breast cancer cells and this activation was greater in the cocultures with HER2-positive TAFs (**Fig. 1I**).

Finally, to show that the coinoculation with HER2-positive TAFs induces resistance to HER2-targeted therapies *in vivo,* we inoculated MDA-MB-453 cells alone or coinoculated with either healthy stromal fibroblasts or HER2-positive TAFs in the CAM of day 11 chicken embryos and treated the tumors for 5 days with lapatinib. Similar to what happened when we coinoculated the cells orthotopically in nude mice (**Fig. 1E**), the tumors derived from the coinoculation with HER2-positive TAFs were bigger (**Fig. 1J**). Interestingly, MDA-MB-453 cells inoculated alone or with RMFs were sensitive to lapatinib and the tumor weight 6 days after inoculation was reduced (**Fig. 1J**). However, MDA-MB-453 cells coinoculated with HER2-positive TAFs were resistant to lapatinib treatment and tumor weight was not altered (**Fig. 1J**). These results support our data indicating that HER2-positive fibroblasts can induce lapatinib resistance in breast cancer cells *in vivo*. Therefore, our results suggest that co-inoculation with HER2-positive TAFs reprograms breast cancer cells into a resistant phenotype by keeping HER2 upregulated and activated.

HER2 oncogene addiction and alternative FGFR2 signaling in breast cancer cell lines resistant to trastuzumab and lapatinib

We hypothesized that soluble factors secreted by HER2-TAFs probably promoted the survival of HER2-positive breast cancer cells by activating alternative compensatory HER2 pathways.

Therefore, to identify new potential targets related to tumor escape from anti-HER2 therapies, we developed a panel of several breast cancer cell lines resistant to trastuzumab and to lapatinib. For this purpose, we selected three cell lines that have different patterns of HER2 overexpression or amplification reflecting the molecular heterogeneity in hormone receptors among patients with breast cancer: MDA-MB-453, which shows HER2 overexpression with no amplification of the 17q chromosome, and BT-474 and SK-BR-3, which both show 17q12 copy number gain.

We developed the resistant phenotypes by continuously exposing the parental wild-type cell lines to increasing concentrations of trastuzumab or lapatinib for 5 months and selecting the resistant population that survived each round of treatment (Supplementary Fig. S1A). To ensure some degree of heterogeneity in the residual population, we adjusted drug doses to avoid reductions in the cell population of more than 80%. To confirm the resistance of the generated cell lines, we performed cell growth assays and clonogenic assays for the parental and resistant cell lines treated with increasing doses of trastuzumab or lapatinib (Supplementary Fig. S3A and S3B).

FISH analysis for *HER2* to identify chromosomal divergences between the parental and resistant cell lines revealed no significant differences in copy number gain among the different cell lines (Supplementary Fig. S3C). Furthermore, the resistant cell lines showed no changes in the expression of estrogen and progesterone receptors (**Table 1**).

To determine whether the drug-resistant cell lines remained dependent on the HER2 pathway, we analyzed HER2 activity under drug pressure (**Fig. 2A–C**). We found that in basal conditions the levels of HER2 phosphorylation in drug-resistant cell lines were similar to those of the parental cell lines (**Fig. 2A–C**; Supplementary Fig. S4A). Interestingly, under drug pressure, all the cell lines overactivated the HER2 pathway (**Fig. 2A–C**; Supplementary Fig. S4A). Staining for total HER2 showed a similar degree of HER2 protein expression in all the cell lines (**Fig. 2B**; Supplementary Fig. S4B and S4C). These results suggest that the trastuzumab-resistant and lapatinib-resistant phenotypes retain *HER2* oncogene addiction.

We also studied the activation of survival and proliferation pathways in parental and resistant cells (Supplementary Fig. S4D). Our results showed that treatment with trastuzumab and lapatinib inhibited AKT activation in parental cells (Supplementary Fig. S4D). However, resistant cells were less sensitive to AKT inhibition (Supplementary Fig. S4D). In addition, treatment with HER2-targeted therapies reduced ERK phosphorylation in resistant cells (Supplementary Fig. S4D). Nevertheless, parental cells seem to be less sensitive to ERK inhibition by lapatinib or trastuzumab (Supplementary Fig. S4D). Therefore, our results suggest that resistant cell lines adapt and keep AKT activated even in the presence of HER2-targeted therapies.

Because the HER2 pathway is still active even when the receptor is being inhibited by specific anti-HER2 drugs, we hypothesized that HER2 activation might be regulated through indirect transactivation. We performed a RTK phospho-protein array (26) to compare phosphorylated RTKs levels in the resistant versus parental cell lines (**Fig. 2D**). We found that several phosphorylated RTKs were notably upregulated in the resistant cell lines. Some of these RTKs [e.g., IGFR (24), HGFR (27), and some EPHRIN receptors (28)] have been related to failure of anti-HER2 therapies, so it seems that our system successfully identified already known mechanisms to promote resistance to anti-HER2 therapies (**Fig. 2D**).

Next, we identified potential receptors to study for each of the two anti-HER2 drug treatments, selecting receptors that were differentially overactivated in at least two of the three resistant cells lines in our model. We identified 13 receptors overactivated in the trastuzumab-resistant cell lines and 7 in the lapatinib-resistant cell lines; 4 of these [fibroblast growth factor receptor 2 (FGFR2), insulin receptor (INSR), Ret proto-oncogene (RET), and kinase insert domain receptor (KDR)] were commonly overactivated in both trastuzumab-resistant and lapatinib-resistant cell lines (**Fig. 2E**). The role of INSR and KDR on trastuzumab resistance had already been described (29, 30). However, there was little literature about the role of FGFR2 and RET in HER2 therapies resistance and because our previous results showed that TAFs were involved in mediating HER2-targeted therapies resistance (**Fig. 1**), we decided to focus on the role of FGFR2 in facilitating TAF-mediated resistance.

To investigate the role of FGFR2 in establishing the drug-resistant phenotype, we first analyzed FGFR2 levels and activation in response to trastuzumab and lapatinib in the different cell lines (**Fig. 2F** and **G**; Supplementary Fig. S4E). We found that the resistant cell lines also expressed higher levels of FGFR2 receptor at the transcript level (**Fig. 2F**). Moreover, in basal conditions lapatinib resistant cell lines express higher levels of phosphorylated FGFR2 than parental cells, suggesting that in the resistant cell lines this pathway is activated even before treatment (**Fig. 2G**; Supplementary Fig. S4E). Furthermore, after trastuzumab and lapatinib treatments, FGFR2 was further activated in both the parental and drug-resistant cell lines (**Fig. 2G**). These results suggest that the resistant cell lines have a higher dependence on the FGFR2 pathway than the parental cell lines.

We explored next whether the cross-talk between fibroblasts and cancer cells was mediated by the activation of the FGFR2 pathway. Therefore, we tested whether treatment of breast cancer cells with fibroblast-conditioned media promotes FGFR2 activation (**Fig. 2H** and **I**; Supplementary Fig. S4F). Exposing MDA-MB-453 parental cells to TAF-conditioned media induced FGFR2 activation, and its activation was greater when the cells were treated with HER2-positive TAF conditioned media (**Fig. 2H** and **I**; Supplementary Fig. S4F). In addition, when we analyzed FGFR2 activation in primary cultures of the tumors that developed from MDA-MB-453 cells coinoculated with

Table 1. Modulation of breast cancer markers with the resistant phenotype.

Cell line	ER	PR	CK5
Parental SK-BR-3	0	0	0
Trastuzumab-resistant SK-BR-3	0	0	0
Lapatinib-resistant SK-BR-3	0	0	0
Parental BT-474	2	2	0
Trastuzumab-resistant BT-474	3	3	0
Lapatinib-resistant BT-474	3	3	0
Parental MDA-MB-453	0	0	0
Trastuzumab-resistant MDA-MB-453	0	0	0
Lapatinib-resistant MDA-MB-453	0	0	0

Abbreviations: CK5, cytokeratin 5; ER, estrogen receptor; PR, progesterone receptor.

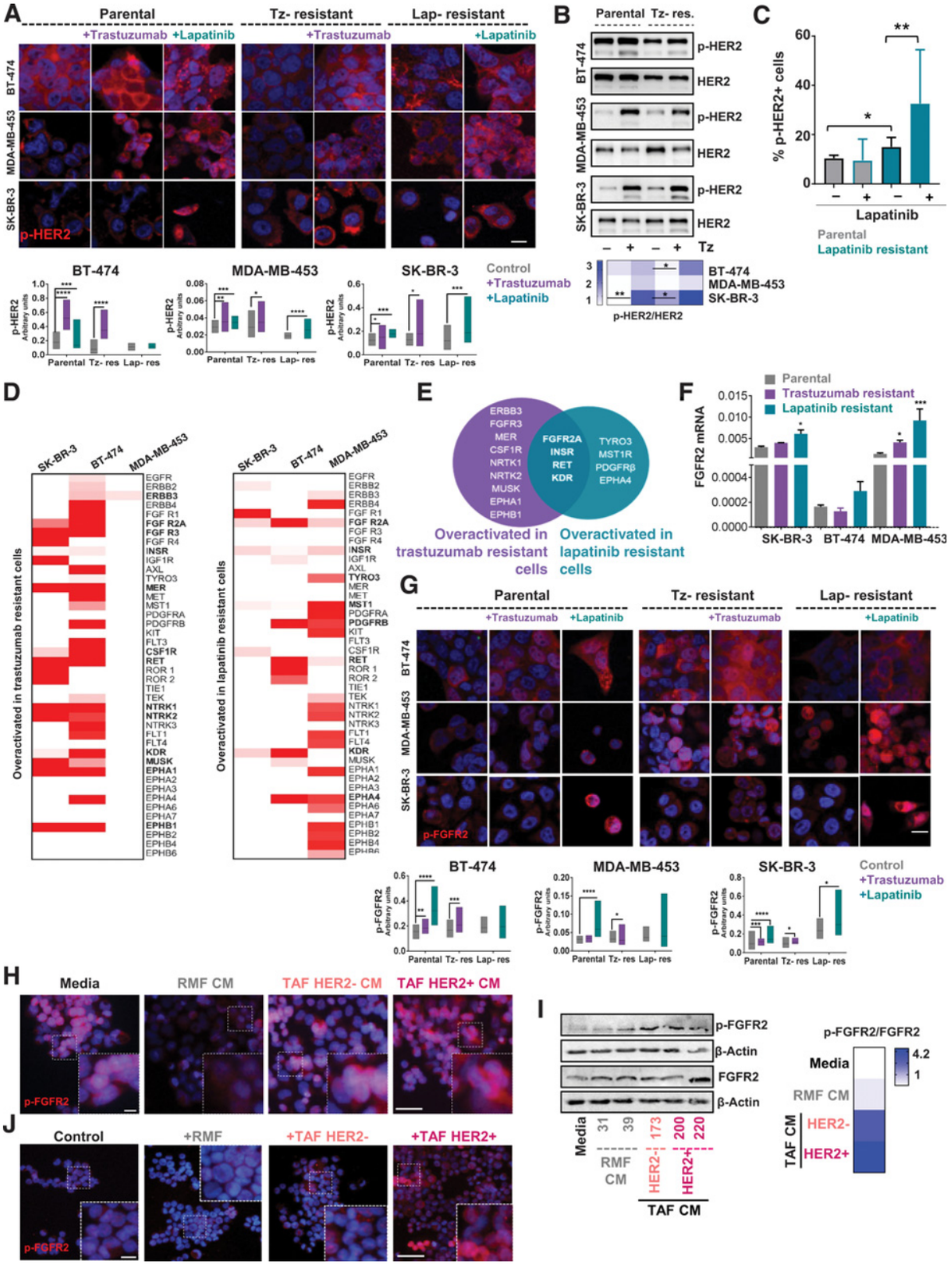

fibroblasts (**Fig. 1E**), we found higher FGFR2 activation in those cells derived from MDA-MB-453 coinjected with HER2-positive TAFs (**Fig. 2J**; Supplementary Fig. S4G), which suggests that the cross-talk between breast cancer cells and HER2-positive TAFs stimulates FGFR2 activation in breast cancer cells.

FGF ligands regulate the survival of trastuzumab and lapatinib-resistant cell lines through activation of FGFR2 pathway and HER2 transactivation by c-Src

To further evaluate the role of fibroblasts in FGFR2 activation, we analyzed the expression of FGFR2 ligands in healthy fibroblasts and TAFs (Supplementary Fig. S5A). We found that *FGF1, FGF2, FGF5, FGF7,* and *FGF9* were upregulated in TAFs at the mRNA level (Supplementary Fig. S5A). We then tested the protein expression of these ligands in healthy stroma fibroblasts and TAFs and found that FGF5 was upregulated in TAFs (**Fig. 3A** and **B**). Interestingly, HER2-positive TAFs express the highest levels of FGF5 (**Fig. 3A** and **B**). Furthermore, using ELISA, we found that HER2-positive TAFs secrete higher levels of FGF5 (**Fig. 3C**) than the other fibroblasts.

Next, we explored the roles of FGF2 and FGF5 in activating FGFR2 and inducing HER2 transactivation and resistance to lapatinib and trastuzumab. First, we treated the resistant MDA-MB-453 cells with FGF2 and FGF5, which, as expected, induced FGFR2 activation (**Fig. 3D**). More interestingly, both FGF2 and FGF5 promoted HER2 activation, both in parental (**Fig. 3E**) and principally in resistant cell lines (**Fig. 3F**). Next, we performed proliferation assays in parental and resistant cell lines pretreated with FGF2 or FGF5 before treatment with trastuzumab and lapatinib (**Fig. 3G** and **H**). In the absence of trastuzumab and lapatinib, treatment with FGF2 and FGF5 only induced proliferation in resistant cell lines (**Fig. 3G** and **H**), suggesting the resistant cells lines are more dependent on FGFR2 signaling for proliferation in basal conditions than the parental cells. In addition, pretreatment with the ligands increased resistance to trastuzumab slightly in trastuzumab resistant cells, but not in parental cell lines (**Fig. 3G**). Interestingly, pretreating the parental and lapatinib resistant cell lines with FGF2 and FGF5 had a protective effect against lapatinib in both parental and resistant cell lines, but the effect was more accentuated in the lapatinib-resistant cells (**Fig. 3H**). These results suggest that FGF2 and FGF5 can induce survival in the presence of anti-HER2–targeted therapies, especially in resistant cell lines. Furthermore, our data suggest that this protective effect is mediated via HER2 transactivation by FGFR2.

We have previously shown that HER2 transactivation by G-protein–coupled receptors can be mediated by c-Src activation (31); hence, we studied whether treatment with FGF ligands or with the fibroblast conditioned media induced c-Src activation in our cells (**Fig. 3I** and **J**).Treatment with FGF2 and FGF5 lead to c-Src activation in resistant cells (**Fig. 3I**). Furthermore, c-Src activation was higher when the cells were treated with FGF5 (**Fig. 3I**). In addition, culturing parental cells with HER2-positive TAFs conditioned media, induced a slight c-Src activation as well (**Fig. 3J**).

To test whether c-Src activation by FGF5 or TAFs conditioned media was responsible for HER2 activation, we pretreated resistant cells with a c-Src inhibitor (4-(4′-phenoxyanilino)-6,7-dimethoxyquinazoline) and then treated them with FGF5 or HER2–positive TAFs conditioned media (**Fig. 3K**; Supplementary Fig. S5B). We found that both FGF5 and HER2-postive TAFs conditioned media induced HER2 and FGFR2 activation (**Fig. 3K**; Supplementary Fig. S5B). However, treatment with a c-Src inhibitor reversed HER2 activation, without affecting FGFR2 activation (**Fig. 3K**; Supplementary Fig. S5B), which suggests that c-Src activation by FGFR2 is partially responsible of HER2 transactivation.

Finally, to assess whether HER2 phosphorylation was dependent on FGFR2 activation, we treated resistant cell lines with two FGFR2 inhibitors, infigratinib and ponatinib. In the resistant cell lines, both

Figure 2.

HER2 oncogene addiction and alternative FGFR2 signaling in breast cancer cell lines resistant to trastuzumab and lapatinib. **A,** Representative images of phospho-HER2 staining (Y1248, phosphorylated levels represented as p-, in red) in SK-BR-3, BT-474, and MDA-MB-453 parental and drug-resistant cells lines (trastuzumab resistant, Tz-resistant, and lapatinib resistant, Lap-resistant) treated with trastuzumab (100 μg/mL) and lapatinib (4 μmol/L) for 72 hours. Scale bar, 50 μm. Bottom, graphs showing activated HER2 (Y1248, phosphorylated) levels quantified as mean fluorescence intensity (MFI). Trastuzumab resistant (Tz-res) and lapatinib resistant (Lap-res). Data, mean ± SD; $n = 3$. **B,** Representative Western blot analysis of phospho-HER2 (Y-1221/22) and total levels of HER2 in SK-BR-3, BT-474, and MDA-MB-453 parental and trastuzumab-resistant cells lines (Tz-res.) treated with trastuzumab (Tz; 100 μg/mL) for 2 hours. Heatmap below shows densitometric quantification of the Western blot analyses, expressed as the ratio of activated versus total HER2 expression relative to the expression of β-actin or α-tubulin. Data, mean ± SD; $n = 3$. **C,** Flow cytometry quantification of the percentage of phospho-HER2–positive cells (Y1248) in SK-BR-3, BT-474, and MDA-MB-453 parental and lapatinib-resistant cell lines treated with lapatinib 1 μmol/L for 72 hours. Data, mean ± SD for all three cell lines, $n = 2$. **D,** Heatmap depicting the relative active status for the 42 RTKs in the study. For each receptor, the mean value of the densitometric quantification in the resistant cell lines was compared with that of the parental cell line. $n = 3$. **E,** Venn diagram representing the RTKs that were overactivated in at least two of the three resistant cell lines to trastuzumab in purple and to lapatinib in green. Intersection shows common RTKs overactivated in both HER2-targeted therapy–resistant models. **F,** FGFR2 qPCR in parental, trastuzumab-resistant, and lapatinib-resistant SK-BR-3, BT-474, and MDA-MB-453 cells. Data, mean ± SD, $n = 3$. **G,** Representative images showing phospho-FGFR2 (Y653-654, phosphorylated levels represented as p-, in red) staining in SK-BR-3, BT-474, and MDA-MB-453 parental and drug-resistant cell lines (trastuzumab resistant, Tz-resistant, and lapatinib resistant, Lap-resistant) treated with trastuzumab (100 μg/mL) and lapatinib (4 μmol/L) for 72 hours. Scale bar, 50 μm. Bottom, graphs showing phosphorylated (Y653-654) FGFR2 level quantification (MFI) of the images in **G**. Trastuzumab resistant (Tz-res) and lapatinib resistant (Lap-res). Data, mean ± SD, $n = 3$. **H,** Representative images showing phospho-FGFR2 (Y653-654, phosphorylated levels represented as p-, in red) staining in parental MDA-MB-453 cell lines cultured for 72 hours with normal media (media) or conditioned media from healthy stroma fibroblasts (RMF CM, RMF-31), HER2-negative TAFs ($HER2^-$ TAF CM, TAF-318), or HER2-positive TAFs ($HER2^+$ TAF CM, TAF-200). Scale bar, 100 μm. Magnification scale bar, 25 μm. **I,** Western blot of phosphorylated (Y769) and total levels of FGFR2 and β-actin in parental MDA-MB-453 cell lines treated for 24 hours with normal media (media) or conditioned media from healthy stroma fibroblasts (RMF CM), HER2-negative TAFs ($HER2^-$ TAF CM), or HER2-positive TAFs ($HER2^+$ TAF CM). Heatmap shows densitometric quantification expressed as the ratio of activated versus total FGFR2 expression relative to the expression of β-actin. The β-actin controls in **Figs. 1B** and **2I** are the same because it is the same experiment and the antibodies were done in the same membrane. Data, mean ± SD, $n = 2$. **J,** Representative images showing phospho-FGFR2 (Y653-654, phosphorylated levels represented as p-, in red) staining in the MDA-MB-453 $mCherry^+$ primary cultures isolated from the tumors derived from the coinoculation of MDA-MB-453 cells alone (control) or with the different fibroblast cell lines: healthy stroma fibroblasts (+RMF31), HER2-negative TAFs (+TAF $HER2^-$ 173), or HER2-positive TAFs (+TAF $HER2^+$ 220; **Fig. 1E**). Scale bar, 50 μm. Magnification scale bar, 25 μm. For FGFR2-activated level quantification, see Supplementary Fig. S4G. *, $P < 0.05$; **, $P < 0.01$. ***, $P < 0.001$; ****, $P < 0.0001$ by ANOVA with Sidak *post hoc* multiple comparison test.

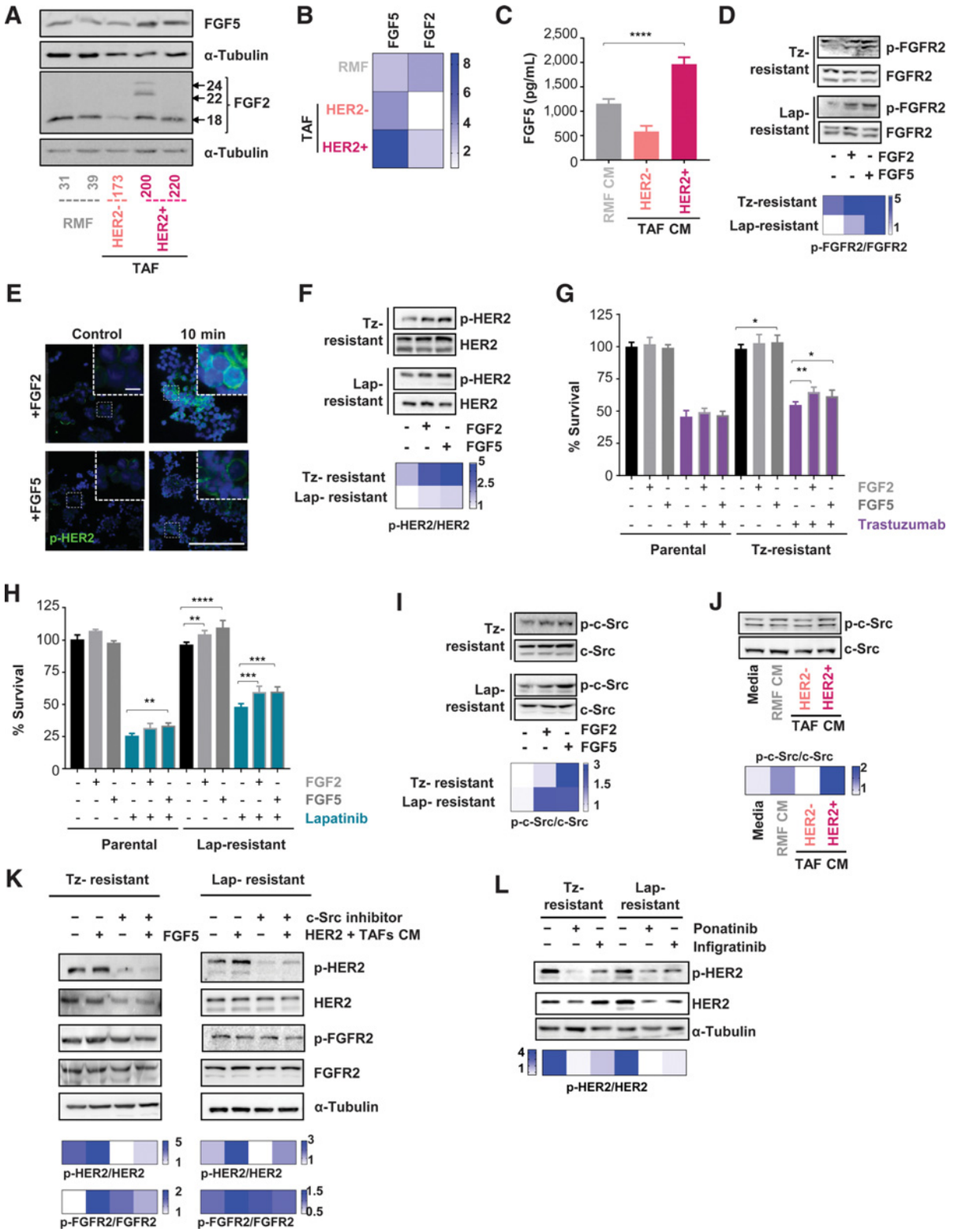

drugs inhibited FGFR2 activation (Supplementary Fig. S5C). We found that FGFR2 inhibition decreased HER2 phosphorylation (**Fig. 3L**; Supplementary Fig. S5D).

The secretome of cells resistant to trastuzumab and lapatinib activates fibroblasts and induces a resistant phenotype in parental cell lines

We next analyzed whether the drug-resistant cell lines also secreted soluble factors able to enhance breast cancer cells' resistance. We found that resistant cells expressed higher levels of FGF5 (**Fig. 4A** and **B**). This suggested that the resistant cell lines might also be able to activate FGFR2 and induce resistance. To test this hypothesis, we treated the parental cell lines with the conditioned media collected from cultures of drug-resistant cell lines and performed proliferation assays in the presence or absence of trastuzumab and lapatinib. Interestingly, exposure to the soluble factors secreted by the drug-resistant cells induced resistance to trastuzumab and lapatinib in parental cells lines (**Fig. 4C**) and induced FGFR2 and HER2 activation (**Fig. 4D** and **E**; Supplementary Fig. S5E and S5F), further suggesting that the resistant cell lines can fuel resistance in a paracrine manner by secreting FGFR2 ligands. We next tested whether the secretome of cell lines resistant to HER2-targeted therapies can affect the phenotype of the fibroblasts. Exposure to the resistant cells conditioned media increased α-SMA and S100A4 expression; the increase was more evident with exposure to conditioned medium from lapatinib-resistant cells (**Fig. 4F**; Supplementary Fig. S5G). Furthermore, treatment of parental cells with the conditioned media of these activated healthy stroma fibroblasts induces resistance to lapatinib and trastuzumab (**Fig. 4G**; Supplementary Fig. S5H), although the effect was more pronounced in the case of lapatinib (**Fig. 4G**). These results suggest that resistant tumor cells can modify their surrounding microenvironment to make it more favorable for their survival and proliferation.

FGFR2 inhibitors reduce tumor progression and reverse resistance to HER2-targeted therapies in trastuzumab-resistant and lapatinib-resistant cells

To further evaluate the role of FGFR2 in resistance, we treated parental and resistant cells with FGFR2 inhibitors and analyzed their effect on survival and apoptosis. We found that as we expected resistant cell lines were more dependent on FGFR2 for survival than parental cell lines and therefore had lower IC_{50}s for FGFR2 inhibitors than parental cell lines (**Fig. 5A**). In addition, trastuzumab- and lapatinib-resistant cell lines were more sensitive to apoptosis induction upon FGFR2 inhibition than parental cells (**Fig. 5B**). These results suggested that the survival of cell lines resistant to trastuzumab and lapatinib depends on FGFR2 pathway activation. Consequently, we tested whether FGFR2 inhibitors could reprogram trastuzumab-resistant and lapatinib-resistant cells to make them sensitive to these treatments. Combination of FGFR2 inhibitors and trastuzumab or lapatinib decreased even more the IC_{50}s, for FGFR2 inhibitors suggesting that inhibition of FGFR2 and HER2 has a synergistic effect (**Fig. 5A**). Furthermore, combination of FGFR2 inhibitors with either lapatinib or trastuzumab potentiated apoptosis in drug-resistant cell lines (**Fig. 5B**). Therefore, combining both FGFR2 inhibitors with trastuzumab and lapatinib resulted in additive cytotoxicity in *in vitro* models in parental and resistant cell lines (**Fig. 5A** and **B**). Nevertheless, the additive effect was always more dramatic in drug-resistant cells (**Fig. 5B**).

To further evaluate the effect of the FGFR2 inhibitors *in vivo*, we inoculated resistant MDA-MB-453 cell lines into the mammary fad pad of athymic nude Foxn 1nu nu/nu mice. Once the tumors reached 100 mm^3, we administered a HER2-targeting agent (trastuzumab or lapatinib) alone, a FGFR2 inhibitor (ponatinib or infigratinib) alone, or a combination of a HER2-targeting agent and a FGFR2 inhibitor. **Figure 5C** shows the growth curves of the tumors derived from drug-resistant cell lines. All treatments reduced tumor growth

Figure 3.

FGF ligands regulate the survival of trastuzumab and lapatinib-resistant cell lines through activation of FGFR2 pathways and HER2 transactivation by c-Src. **A,** Representative Western blot analysis of FGF2 and FGF5 levels in fibroblasts from healthy stroma (RMF31, RMF39) and TAFs derived from HER2-negative breast cancer tumors (TAF $HER2^-$ 173) or HER2-positive tumors (TAF $HER2^+$ 200 and 220). **B,** Heatmap depicting densitometric quantification of FGF5 and FGF2 expression relative to the expression of α-tubulin of the Western blot analysis in **A**. Data, mean ± SD, $n = 2$. **C,** FGF5 levels measured by ELISA in healthy stroma fibroblast (RMF) and TAFs derived from HER2-negative breast cancer tumors (TAF $HER2^-$) or HER2-positive tumors (TAF $HER2^+$). Data, mean ± SD, $n = 3$. **D,** Western blot analysis of phosphorylated (Y769) and total levels of FGFR2 in trastuzumab (Tz-) and lapatinib (Lap-) resistant MDA-MB-453 cell lines treated with FGF2 and FGF5 (100 ng/mL) for 5 minutes. Heatmap below shows densitometric quantification of the ratio of activated versus total FGFR2 expression normalized with β-actin or α-tubulin. Data, mean ± SD. **E,** Representative images showing activated HER2 (Y1248, phosphorylated levels represented as p-, in green) staining in parental MDA-MB-453 cells treated with FGF2 and FGF5 (100 ng/mL) for 10 minutes. Scale bar, 200 μm. Magnification scale bar, 50 μm. **F,** Western blot analysis of phosphorylated (Y-1221/22) and total levels of HER2 in trastuzumab (Tz-) and lapatinib (Lap-) resistant MDA-MB-453 cell lines treated with FGF2 and FGF5 for 5 minutes. Heatmap below shows densitometric quantification of the ratio of activated versus total HER2 expression normalized with β-actin or α-tubulin. Data, mean ± SD, $n = 2$. **G,** Quantification of cell viability represented as percentage of survival of MDA-MB-453 parental and trastuzumab (Tz-)-resistant cells after pretreatment with FGF2 and FGF5 ligands (100 ng/mL) for 24 hours and consecutive treatment with trastuzumab (100 μg/mL) for 48 hours. Data, mean ± SD, $n = 3$. **H,** Quantification of cell viability represented as percentage of survival of MDA-MB-453 parental and lapatinib (Lap-)-resistant cells after pretreatment with FGF2 and FGF5 ligands (100 ng/mL) for 24 hours and consecutive treatment with lapatinib (1 μmol/L) for 48 hours. Data, mean ± SD, $n = 3$. **I,** Western blot analysis of phosphorylated (Y-416) and total levels of c-Src in trastuzumab (Tz-) and lapatinib (Lap-)-resistant MDA-MB-453 cell lines treated with FGF2 and FGF5 ligands (100 ng/mL) for 5 minutes. Heatmap below shows densitometric quantification of the ratio of activated versus total c-Src expression normalized with β-actin or α-tubulin. Data, mean ± SD. **J,** Western blot analysis of phosphorylated (Y-416) and total levels of c-Src in parental MDA-MB-453 cell lines treated with normal media (media) or conditioned media from healthy stroma fibroblasts (RMF 39 CM), HER2-negative TAFs ($HER2^-$ TAF 173 CM), or HER2-positive TAFs ($HER2^+$ TAF 200 CM) for 24 hours. Heatmap below shows densitometric quantification of the ratio of activated versus total c-Src normalized with of α-tubulin. Data, mean ± SD, $n = 2$. **K,** Western blot analysis of phosphorylated and total levels of HER2 (Y1221/1222) and FGFR2 (Y769) in MDA-MB-453 trastuzumab (Tz-) and lapatinib (Lap-)-resistant cell lines pretreated with a c-Src inhibitor (1 μmol/L) for 2 hours and then treated with FGF5 (100 ng/mL) for 6 hours (trastuzumab resistant) or with the conditioned media from $HER2^+$ TAFs for 24 hours (lapatinib resistant). Heatmap below shows densitometric quantification of the ratio of activated versus total HER2 and FGFR2 expression normalized with β-actin or α-tubulin. Data, mean ± SD, $n = 3$. **L,** Western blot analysis of the phosphorylated and total levels of HER2 (Y1221/1222) in trastuzumab (Tz-) and lapatinib (Lap-)-resistant MDA-MB-453 cell lines treated with FGFR2 inhibitors (ponatinib and infigratinib, 2 μmol/L for 24 hours). Heatmap below shows densitometric quantification of the ratio of activated to total HER2 expression normalized with α-tubulin. Data represent, ± SD, $n = 3$. *, $P < 0.05$; **, $P < 0.01$; ***, $P < 0.001$; ****, $P < 0.0001$ by ANOVA with Sidak *post hoc* multiple comparison test.

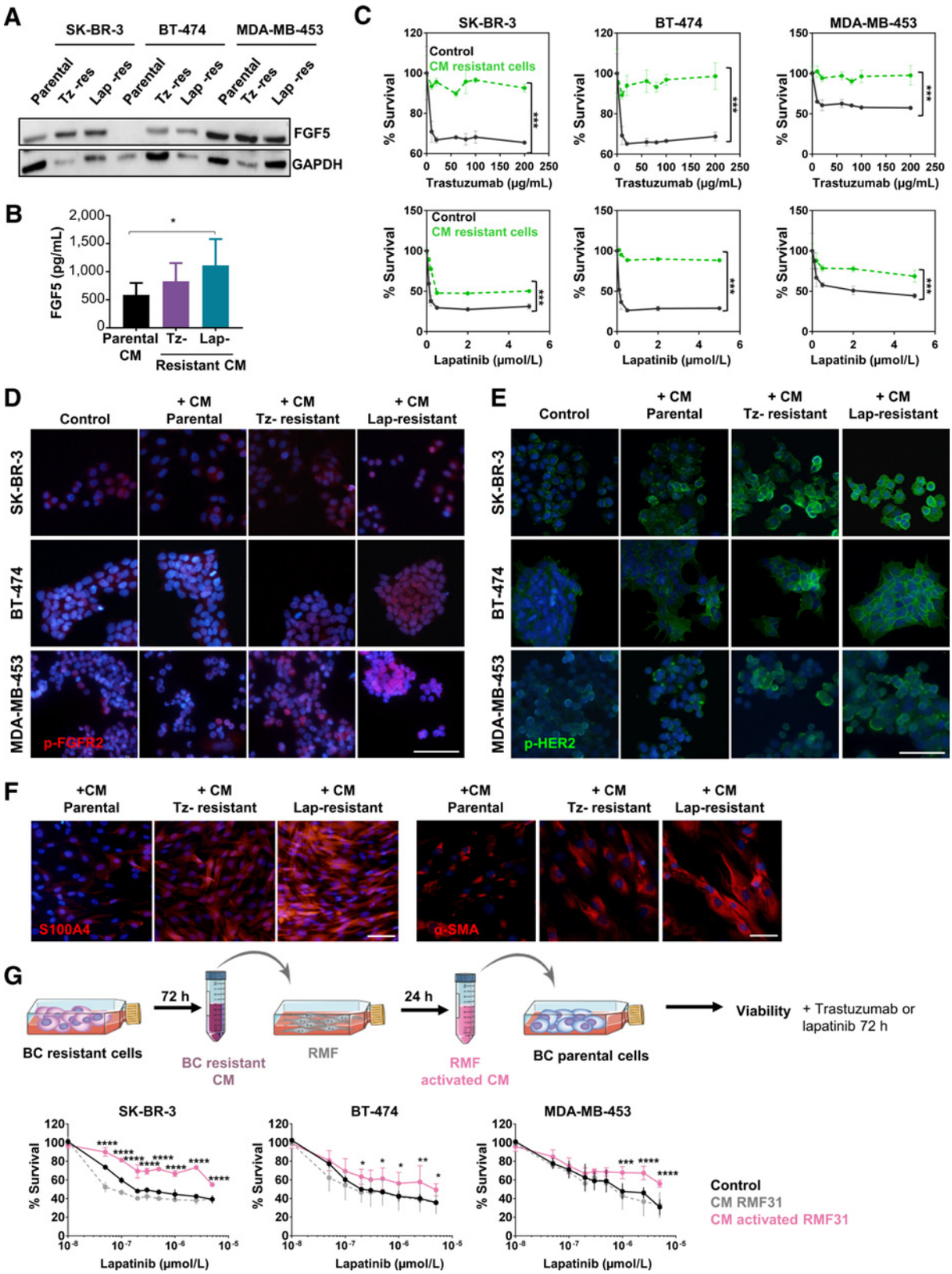

significantly (**Fig. 5C**). Interestingly, in the tumors derived from resistant cell lines, both FGFR2 inhibitors administered alone decreased cell survival and tumor size more than the anti-HER2 drugs administered alone, suggesting that FGFR2 is a significant driver of proliferation and survival in resistant cells (**Fig. 5C**; Supplementary Fig. S5I).

Furthermore, we found that adding FGFR2 inhibitors makes HER2-targeting therapies more effective. In both drug-resistant models, combined treatments were the most effective (**Fig. 5C**; Supplementary Fig. S5I). Moreover, although treatment with FGFR2 inhibitors had little effect on HER2 expression, administration of trastuzumab or lapatinib together with FGFR2 inhibitors consistently resulted in greater inhibition of HER2 expression (**Fig. 5D**). In addition, administering FGFR2 inhibitors reduced infiltration by fibroblasts, and the reduction was greater when FGFR2 inhibitors were combined with trastuzumab or lapatinib (**Fig. 5E**).

Moreover, treatment with FGFR2 inhibitors reversed the resistance to trastuzumab and lapatinib that was induced by the fibroblast-conditioned media (**Fig. 5F**). These results are further evidence of the important role of fibroblasts in maintaining resistance to HER2-targeting therapies. Altogether, our results indicate that HER2-positive TAFs produce higher levels of FGFR2 ligands, which activate FGFR2 and mediate breast cancer cells' resistance to trastuzumab and lapatinib through HER2 transactivation.

Prevalence of TAFs, FGF5, FGFR2, c-Src, and activated HER2 and c-Src expression in human HER2-positive breast cancer

To determine the clinical relevance of the TAFs/ FGFs/ FGFR2/ c-Src triggered resistance mechanism described, we first analyzed the levels of FGFR2 by IHC in a cohort of breast cancer specimens (Supplementary Fig. S6A). We found that 83% of the HER2-positive tumors expressed elevated levels of FGFR2, while among the HER2-negative tumors only 50% of the samples had high FGFR2 expression; hence, HER2-positive tumors expressed higher levels of FGFR2 when compared with HER2-negative tumors (Supplementary Fig. S6B), suggesting that HER2 overexpression in breast cancer might be linked to higher FGFR2 expression.

To further confirm our previous results showing the important role of TAFs/FGF5/FGFR2–mediated HER2 transactivation in breast cancer resistance to trastuzumab and lapatinib, we also investigated the expression and clinical significance of TAF infiltration (α-SMA), FGF5, FGFR2, and phospho-HER2 expression in a cohort of 456 patients. IHC detections of FGF5, α-SMA, FGFR2, and phospho-HER2 are shown in **Fig. 6A**. The analysis of αSMA and FGF5 showed TAFs infiltrating throughout the tumor and FGF5 expression predominantly in the tumor stroma, as expected (**Fig. 6A**). Meanwhile, FGFR2 and phospho-HER2 expression were mainly restricted to tumor cells (**Fig. 6A**). The expression of all the markers was heterogeneous and varied among the samples (**Fig. 6A**). We selected the HER2-positive patients and quantified the percentage of tumor area infiltrated with fibroblasts and the expression of FGF5, FGFR2, and phospho-HER2 and correlated this with the clinical information. Interestingly, when we analyzed the prognosis of HER2-positive patients, we found that high TAF infiltration, high FGF5 stromal expression, high FGFR2 expression, and high HER2 phosphorylation correlated with worse overall survival (**Fig. 6B**) and disease-free survival (DFS; Supplementary Fig. S6C), suggesting that in HER2 breast cancer TAF infiltration, and the overexpression of FGF5 in tumor stroma, as well as expression of FGFR2 in tumor cells together with HER2 activation contribute to poor outcome. Moreover, these findings support our previous results showing that TAFs produce FGF5, which in turn activates FGFR2, leading to HER2 transactivation and a more aggressive behavior. To test our hypothesis that FGFR2 transactivation of HER2 was mediated by c-Src, we also analyzed the expression of c-Src and phospho-c-Src in our cohort of patients with breast cancer (Supplementary Fig. S6D). The expression of c-Src and phospho-c-Src were mainly restricted to tumor cells as expected (Supplementary Fig. S6D). Their expression was heterogeneous and varied among the samples (Supplementary Fig. S6D). When we analyzed HER2 positive and HER2 negative patients, we found almost all HER2-negative patients express low levels of c-Src and phospho-Src (Supplementary Fig. S6E). Interestingly, in HER2-positive patients there is a correlation between c-Src activation and HER2 activation but only when FGF5 and FGFR2 are also upregulated (c-Src, $P = 0.061$; p-Src: $P = 0.001$; **Fig. 6C**). These results confirm our *in vitro* data and supports our hypothesis that in HER2-positive patients, production of FGF5 by fibroblasts induces FGFR2 activation, which phosphorylates c-Src, which itself transactivates HER2, inducing resistance to HER2-targeted therapies.

FGF5 stromal expression and HER2 activation in tumor cells determine response to adjuvant trastuzumab in patients with HER2-positive breast cancer

To test in patients if the transactivation of HER2 by c-Src/FGFR2/ FGF5 leads to resistance to HER2 targeted therapies, we next analyzed

Figure 4.

The secretome of cells resistant to trastuzumab and lapatinib activates fibroblasts and induces a resistant phenotype in parental cell lines. **A,** Western blot analysis showing FGF5 levels in parental, trastuzumab-resistant (Tz-res), and lapatinib-resistant (Lap-res) SK-BR-3, BT-474, and MDA-MB-453 cells. **B,** FGF5 levels measured by ELISA in parental, trastuzumab (Tz-), and lapatinib (Lap)-resistant MDA-MB-453 cells. Data, mean ± SD; $n = 3$. **C,** Cell viability after treating parental SK-BR-3, BT-474, and MDA-MB-453 cells for 72 hours with increasing doses of trastuzumab (0–200 μg/mL, top) and lapatinib (0–5 μmol/L, bottom), in the presence (green lines) or absence (black lines) of conditioned media (CM) derived from resistant cell lines (conditioned media collected after 72 hours of culture). Data, mean ± SD, $n = 3$. **D,** Representative images showing phospho-FGFR2 (Y653-654 phosphorylated levels represented as p-, in red) staining, in parental SK-BR-3 (top), BT-474 (middle), and MDA-MB-453 (bottom), after incubation with the conditioned media (CM) from parental, trastuzumab (Tz-), and lapatinib (Lap-)-resistant cell lines for 72 hours. Scale bar, 200 μm. For FGFR2-activated level quantification, see Supplementary Fig. S5E. **E,** Representative images showing phospho-HER2 (Y1248, phosphorylated levels represented as p-, in green) staining, in parental SK-BR-3 (top), BT-474 (middle), and MDA-MB-453 (bottom) treated as described in **D**. Scale bar, 200 μm. For HER2-activated level quantification, see Supplementary Fig. S5F. **F,** Representative images showing α-SMA (right) and S100A4 (left) staining, in healthy stroma fibroblasts, RMF-31, cultured for 72 hours with conditioned media (CM) from parental, trastuzumab- (Tz), and lapatinib (Lap)-resistant cell lines. Scale bar, 50 μm. **G,** Conditioned media from drug-resistant cell lines were collected after 72 hours and used to treat healthy stroma fibroblast RMF-31. Twenty-four hours later, the conditioned media from these fibroblasts were collected and used to treat parental cells for 72 hours in the presence or absence of increasing doses of lapatinib (0–5 μmol/L). The graphs below show the percentage of survival of SK-BR-3 (left graph), BT-474 (middle graph), and MDA-MB-453 (right graph) cells treated with control media (black line), conditioned media from healthy stroma fibroblasts (gray line), or conditioned media from healthy stroma fibroblasts pretreated with lapatinib-resistant cell line conditioned media (light pink line). Data, mean ± SD, $n = 3$. *, $P < 0.05$; **, $P < 0.01$; ***, $P < 0.001$; and ****, $P < 0.0001$ by ANOVA with Sidak *post hoc* multiple comparison test.

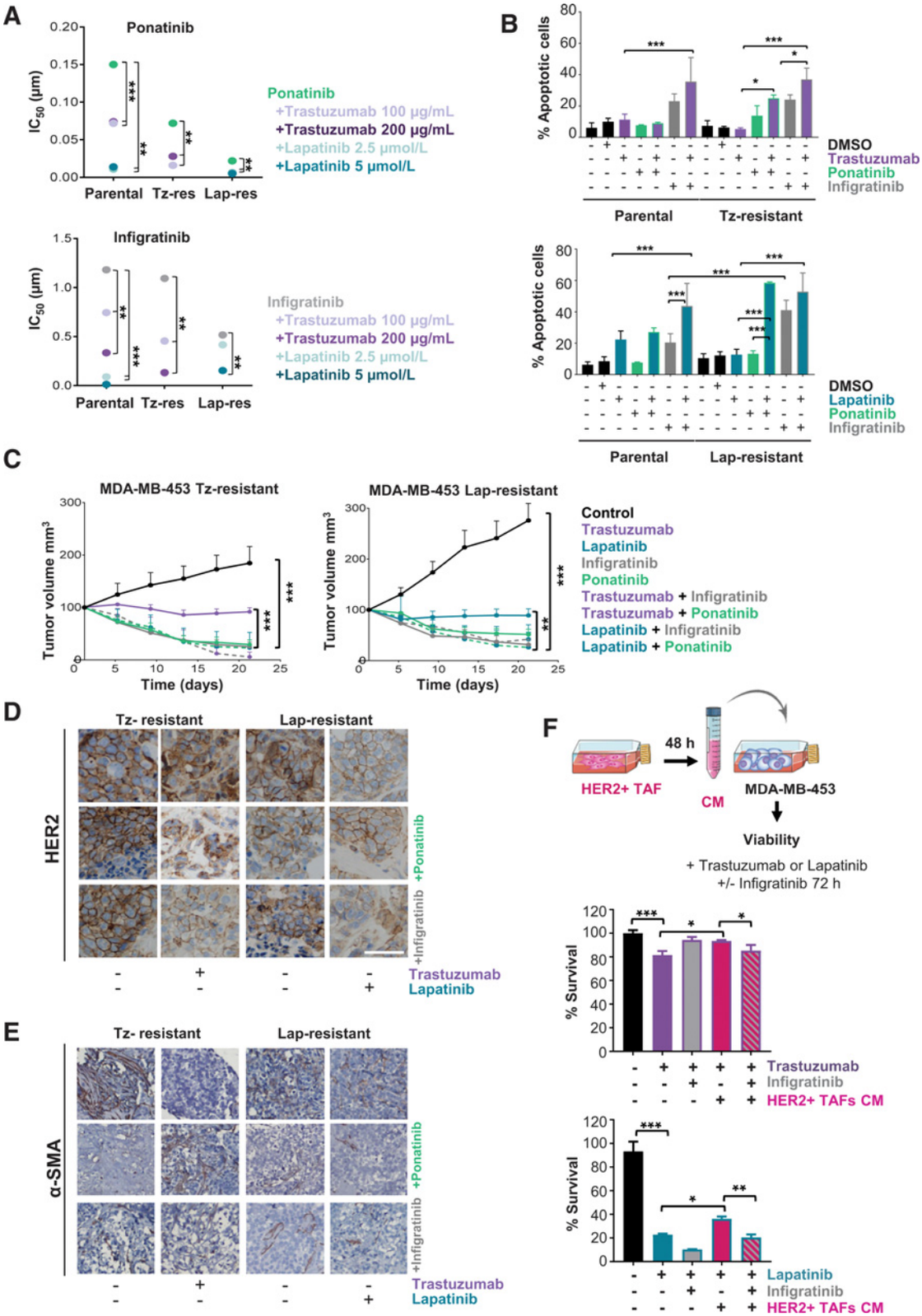

the stromal overexpression of FGF5 and its relationship with HER2 activation. For this, we calculated the prediction of pathologic complete response (pCR) in a cohort of HER2 early breast cancer treated with trastuzumab-containing neoadjuvant therapy. We found that 70% of the patients with pCR expressed low levels of FGF5 ($P = 0.04$; Supplementary Fig. S6F), suggesting that its expression could be used as a biomarker to predict which patients will response poorly to trastuzumab. Interestingly, the levels of phospho-HER2 alone could not predict the pCR ($P = 0.069$; Supplementary Fig. S6G). These observations prompted us to analyze the predictive value of combined, FGF5 and phopho-HER2, using a "CPscore" in which score 0 was defined by those patients with breast cancer with low levels of both FGF5 and phospho-HER2 and score 1 for those with high FGF5 and high phospho-HER2 and correlated it with the clinical data. Interestingly, high CPscore was found in those patients who relapsed ($P = 0.004$; **Fig. 6D**). In addition, the subgroup of patients with high CPscore showed a substantially shorter DFS ($P = 0.001$; **Fig. 6E**). Therefore, patients with HER2-positive early breast cancer with low FGF5 and phospho-HER2 expression in their tumors benefited from trastuzumab treatment, whereas patients with high FGF5 and high phospho-HER2 expression did not.

These results further corroborate our *in vitro* and *in vivo* results and highlight the importance of TAFs/ FGF5/ FGFR2/c-Src in HER2 breast cancer progression and resistance to trastuzumab (**Fig. 6F**). Furthermore, these data suggest that FGF5 and phospho-HER2 expression could be used as biomarkers in the clinic to predict resistance to HER2-targeted therapies. The clinical data further validate our model that TAFs contribute to HER2-targeted therapies resistance in HER2 breast cancer through FGF5-mediated FGFR2 activation (**Fig. 6F**). These findings may help to optimize the adjuvant treatment of patients with HER2-positive breast cancer in the future.

Discussion

We have demonstrated that HER2-positive TAFs secrete soluble factors, such as FGF5, that are able to switch the phenotype of HER2-positive breast cancer cells from sensitive to resistant to trastuzumab and lapatinib. Our results about TAFs contributing to lapatinib resistance in breast cancer, are in agreement with a recent report from Marusyk and colleagues, where they found that 3D coculture of fibroblasts and breast cancer cells strongly protects carcinoma cells from lapatinib (32), as well as with another study where the authors found that fibroblasts promote lapatinib resistance in esophageal cancer (33), reinforcing the idea that fibroblasts are important contributors to the establishment of the lapatinib-resistant phenotype in different cancer types. FGFR2 activation was mediated by fibroblasts' production of FGF1, FGF7, and FGF10 in their study and by FGF2 and FGF5 in ours, possibly because fibroblasts in different cancers might produce different ligands. Our results also agree with those recently reported by Mao and colleagues, who reported that TAFs can induce trastuzumab resistance in HER2-positive breast cancer cells by expanding the cancer stem cell population and activating several signaling pathways such as NFkB, JAK/STAT3, and PI3K/AKT (34).

Moreover, we have also shown that the clinical effects of HER2-targeting therapies can be attenuated by TAFs activating HER2. In agreement with this, some preclinical models found that *HER2* gene amplification is maintained in trastuzumab-resistant clones (35). Furthermore, current clinical data supports that trastuzumab-resistant tumors remain dependent on HER2 pathways to survive, even in advanced stages (36). We propose that in these resistant tumors, selective pressure leads to compensations in alternative RTK signaling that enable them to continue growing. Our phosphoproteomic assays, cell line assays, and xenografts showed that FGFR2 was overactivated in cell lines resistant to trastuzumab and lapatinib and induced HER2 transactivation. This is in agreement with several studies that have shown that there is a correlation between HER2 amplification and FGFR2 activation (37–40). Furthermore, Wei et al has previously described that FGFR2 activates the metalloprotease ADAM10 that promotes intracellular accumulation of the truncated p95HER2 protein, which leads to enhanced HER2 signaling and diminished sensitivity to trastuzumab in breast cancer (41), which is in agreement with our results. In our system, we did not observe an upregulation of p95HER2, but we did not use specific antibodies for it and the cell lines and conditions for FGFR2 activation were different, so we cannot rule out that metalloproteases might also be playing a role in HER2 transactivation. More experiments will be necessary to test whether ADAM10 is involve in HER2 transactivation by FGFR2 in our model. Nevertheless, we have described an alternative mechanism for FGFR2-mediated transactivation of HER2. In our model, HER2 transactivation by FGFR2 was mediated by c-Src kinase activation. c-Src is a non-receptor tyrosine kinase involved in signaling and cross-talk between growth-promoting pathways (42). It has previously been

Figure 5.

FGFR2 inhibitors reduce tumor progression and reverse resistance to HER2-targeted therapies in trastuzumab-resistant and lapatinib-resistant cells. **A,** Parental, trastuzumab-resistant (Tz-res), and lapatinib-resistant (Lap-res) MDA-MB-453 cells IC_{50} (95% confidence interval for each treatment) for ponatinib (top) and infigratinib (bottom), in the presence or absence of different doses of trastuzumab (100 and 200 μg/mL) or lapatinib (2.5 and 5 μmol/L). $n = 3$. **B,** Percentage of apoptotic Annexin V–positive cells in parental and drug-resistant MDA-MB-453 cells [top, trastuzumab (Tz-) resistant and bottom, lapatinib (Lap-) resistant] treated for 72 hours with trastuzumab (100 μg/mL), lapatinib (1 μmol/L), ponatinib (0.05 μmol/L), and infigratinib (0.5 μmol/L) alone or in a combination of an anti-HER2 drug with a FGFR2 inhibitor. Data, mean ± SD, $n = 3$. **C,** Tumor growth of orthotopically implanted MDA-MB-453 [trastuzumab-resistant (Tz-resistant) cells (left graph) and lapatinib-resistant (Lap-resistant) cells (right graph) treated with trastuzumab (10 mg/kg), lapatinib (10 mg/kg), infigratinib (10 mg/kg), or ponatinib (10 mg/kg)], or a combination of an anti-HER2 drug and an FGFR2 inhibitor for 21 days. The data are expressed as decrease in tumor volume reduction using treatment day 0 as a reference. Data, mean ± SD, $n = 5$. **D,** Representative images showing HER2 staining in tumors from MDA-MB-453 trastuzumab-resistant (Tz-resistant) cells and lapatinib-resistant (Lap-resistant) cells treated with trastuzumab (Tz; 10 mg/kg), lapatinib (Lap; 10 mg/kg), ponatinib (10 mg/kg), or infigratinib (10 mg/kg), or a combination of an anti-HER2 drug and an FGFR2 inhibitor for 21 days. Scale bar, 50 μm. **E,** Representative images showing α-SMA staining in tumors from MDA-MB-453 trastuzumab-resistant (Tz-resistant) cells and lapatinib-resistant (Lap-resistant) cells treated as described in **D**. Scale bar, 50 μm. **F,** HER2-positive TAFs were cultured for 48 hours, and the conditioned media were collected and used to treat parental MDA-MB-453 cells for 72 hours in the presence of infigratinib (2 μmol/L) alone or in combination with trastuzumab (200 μg/mL) or lapatinib (6.25 μmol/L). The graphs show percentage of survival in the cells treated with either HER2-positive TAF conditioned media ($HER2^+$ TAF CM), infigratinib, or both in the presence of trastuzumab (top) or lapatinib (bottom). Data, mean ± SD, $n = 3$. *, $P < 0.05$; **, $P < 0.01$; ***, $P < 0.001$; and ****, $P < 0.0001$ by ANOVA with Sidak *post hoc* multiple comparison test.

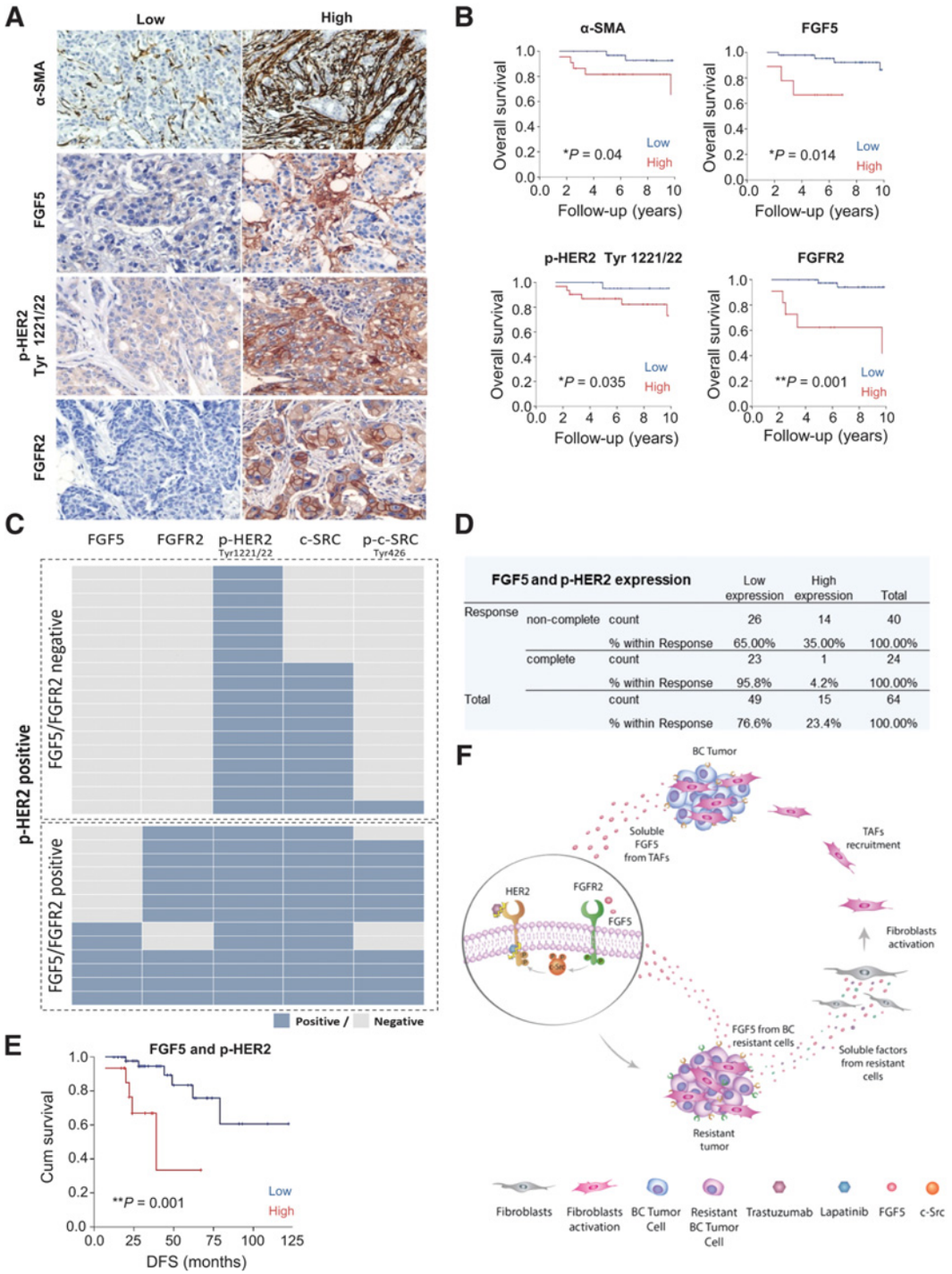

Figure 6.

Prevalence of TAFs, FGF5, FGFR2, c-Src, and activated HER2 and c-Src expression in human HER2-positive breast cancer. **A,** Representative images showing low and high levels of stromal αSMA (first row) and FGF5 (second row) expression and activated levels of HER2 (Y1221/22; third row) and total FGFR2 (fourth row) expression in tumor cells from patient samples. Scale bar, 100 μm. **B,** Kaplan–Meier analyses of overall survival (OS) in a cohort of patients with HER2$^+$ breast cancer stratified by αSMA (first graph), FGF5 (second graph), phospho-HER2 (third graph), or FGFR2 (fourth graph) expression. **C,** Association of c-Src and phospho-c-Src (Y416) expression with FGF5/ FGFR2 and phospho-HER2 expression in HER2-positive patients. **D,** Association of FGF5 and phospho-HER2 (Tyr 1221/22; p-HER2) expression with clinical data in a cohort of 64 HER2$^+$ patients treated with trastuzumab in neoadjuvance. **E,** Kaplan–Meier analyses of DFS in a cohort of 64 patients with HER2$^+$ breast cancer stratified by high or low coexpression of FGF5 and phospho-HER2 (Tyr 1221/22; p-HER2). **F,** Scheme of the proposed role of TAFs in inducing breast cancer resistance to anti-HER2–targeted therapies. HER2$^+$ breast cancer cells recruit healthy stroma fibroblasts and activate them. Those TAFs produce FGF5 that will activate FGFR2 in breast cancer cells, which will transactivate HER2 trough c-Src activation, promoting cell survival and proliferation, leading to breast cancer cell resistance to HER2-targeted therapies.

shown that FGFR2 can induce c-Src activation (43). Although direct binding between FGFR2 and c-Src has not been demonstrated, recent evidence has shown that FRS2 activation by FGFR2 bridges this interaction (44, 45). Moreover, we have previously shown that HER2 transactivation by G-coupled protein receptors was partially dependent on c-Src activation (31). In our resistant cell lines FGF5 and HER2-positive TAFs conditioned media induction of HER2 was dependent on c-Src activation. Interestingly, our clinical data shows that phospho-c-Src expression correlates with FGF5, FGFR2 and p-HER2 expression in HER2-positive patients. Therefore, c-Src mediates TAFs-FGF5 pro-survival functions by bridging FGFR2-HER2 cross-talk in trastuzumab- and lapatinib-resistant breast cancer cells.

Furthermore, our *in vivo* and *in vitro* data show that pharmacologic inhibition of FGFR2 reverses HER2 activation in all cell lines and induces apoptosis in the trastuzumab-resistant and lapatinib-resistant cell lines. Moreover, we have shown that combining trastuzumab or lapatinib with FGFR2 inhibitors is effective in overcoming resistance to HER2-targeting therapies in *in vitro* and *in vivo* models. This suggests that FGFR2 is a plausible molecular target for overcoming trastuzumab and lapatinib resistance. These results are in agreement with previous reports that have shown that FGFR inhibitors can revert HER2-targeted therapies resistance in different cancers (33, 38, 46, 47). Yu and colleagues have recently described that miR-494 downregulates the protein expression of FGFR2 and reverts lapatinib resistance by inhibiting the formation of cancer initiating cells (38). Piro and colleagues have shown that in gastric cancer, activation of FGFR3 drives AKT pathway activation and is responsible for trastuzumab resistance (48). Hanker and colleagues have shown that amplification of FGFR signaling promotes resistance to HER2 inhibition (47). In their study, they showed that FGF4/FGFR signaling can bypass HER2 inhibition and activate the ERK pathway (47). All these studies further support our conclusion that TAFs secretion of FGF5 can drive resistance to HER2 inhibitors through activation of FGFR2 signaling. Our findings agree also with those reported by Azuma and colleagues, who found that FGFR2 was involved in resistance to lapatinib in UACC812 cells, although in their study the *FGFR2* gene was highly amplified and correlated with reduced expression of HER2 (46). In contrast, in our study, resistant cell lines continued to depend on HER2 signaling, and FGFR2 activation by FGF5 induced HER2 transactivation via c-Src activation.

In addition, our clinical results revealed that in patients with HER2-positive breast cancer, TAF infiltration, stromal expression of FGF5 as well as tumor cell FGFR2 overexpression and HER2 activation correlate with c-Src activation and worse prognosis and can predict clinical outcome. Furthermore, we found that in a cohort of trastuzumab-treated patients, those patients with high FGF5 stromal expression and high levels of HER2 phosphorylation would not benefit from trastuzumab neoadjuvant treatment. Therefore, our findings indicating that FGF5 activation of HER2 via FGFR2 can promote resistance to HER2 inhibitors are potentially applicable to a significant cohort of patients with HER2-positive breast cancer and could directly impact the clinical management of these patients. Furthermore, FGF5 and phospho-HER2 have the potential to be used as biomarkers to predict resistance to HER2-targeted therapies.

Finally, our results highlight the essential contribution of the stroma in resistance to HER2-targeted therapies and the potential utility of focusing on the FGFR2 pathway in breast cancers resistant to HER2-targeting drugs; this strategy might overcome resistance by targeting both resistant clones that overexpress FGFR2 to maintain HER2-driven survival and genetically stable fibroblasts inducing and maintaining the resistant phenotype.

Disclosure of Potential Conflicts of Interest

F. Rojo reports receiving speakers bureau honoraria from Roche, AstraZeneca, Bristol-Myers Squibb, and MSD, and is an advisory board member/unpaid consultant for Roche, AstraZeneca, and MSD. A. Bill and L.A. Gaither are employees/paid consultants for Novartis. A. Lluch reports receiving commercial research grants from Amgen, AstraZeneca, Boehringer-Ingelheim, GlaxoSmithKline, Novartis, Pfizer, Roche-Genentech, Eisai, Celgene, and Pierre Fabre, and other remuneration from Novartis, Pfizer, Roche/Genentech, Eisai, and Celgene. J. Albanell reports receiving speakers bureau honoraria from Roche. No potential conflicts of interest were disclosed by the other authors.

Authors' Contributions

Conception and design: P. Fernández-Nogueira, V. Almendro, F. Rojo, P. Gascon, P. Bragado

Development of methodology: P. Fernández-Nogueira, M. Mancino, G. Fuster, A. López-Plana, P. Jauregui, V. Almendro, E. Enreig, S. Menéndez, F. Rojo, A. Noguera-Castells, L.A. Gaither, L. Serrano, L. Recalde-Percaz, N. Moragas, R. Alonso, E. Ametller, P. Gascon

Acquisition of data (provided animals, acquired and managed patients, provided facilities, etc.): P. Fernández-Nogueira, S. Menéndez, F. Rojo, A. Bill, L.A. Gaither, L. Serrano, A. Lluch

Analysis and interpretation of data (e.g., statistical analysis, biostatistics, computational analysis): P. Fernández-Nogueira, V. Almendro, F. Rojo, A. Bill, L.A. Gaither, L. Serrano, P. Gascon, P. Bragado

Writing, review, and/or revision of the manuscript: P. Fernández-Nogueira, M. Mancino, V. Almendro, F. Rojo, A. Bill, L.A. Gaither, A. Rovira, A. Lluch, J. Albanell, P. Gascon, P. Bragado

Administrative, technical, or material support (i.e., reporting or organizing data, constructing databases): P. Fernández-Nogueira, S. Menéndez, F. Rojo, L.A. Gaither, A. Rovira, P. Gascon

Study supervision: P. Fernández-Nogueira, V. Almendro, L.A. Gaither, J. Albanell, P. Gascon, P. Bragado

Acknowledgments

The authors thank Darya Kulyk for her help preparing the schemes that are shown in the figures and for the preparation of the graphical abstract and the summary scheme in Fig. 6F. They also thank Inga Hansine Rye and Hege Elisabeth Giercksky (Institute for Cancer Research, Oslo University Hospital Radiumhospitalet, Oslo, Norway) for their help in optimizing some of the techniques used in the project. This work was performed at IDIBAPS (CERCA Programme/Generalitat de Catalunya). This work was supported by grants from Cellex Foundation, FROI Foundation, Instituto de Salud Carlos III through the projects PI18/00382, PI15/00661, PIE15/00008, PI15/00146, PI15/00934, PI15/01617, PI18/00006, CIBERONCO CB16/12/00241 and RTICC, RD12/00360055, and RD12/0036/0070 (cofunded by European Regional Development Fund) -Investing in your future-", Secretaria d'Universitats i Recerca del Departament d'Economia i Coneixement (2014_SGR_530, 2014_SGR_740, 2017_SGR_1305 and 2017 _SGR _507) and BBVA (becas Leonardo 2018, BBM-TRA-0041). MARBiobanc is supported by ISCiii/FEDER (PT17/0015/0011) and the "Xarxa de Bancs de tumors" sponsored by Pla Director d' Oncologia de Catalunya (XBTC). P. Bragado has been funded by a Beatriu Pinos postdoctoral fellowship "AGAUR; BP-B 00160" (cofunded by European Union). P. Fernández-Nogueira, E. Enreig, and A. Noguera-Castells have been funded by APIF fellowships from the University of Barcelona, School of Medicine. M. Mancino is supported by the Sara Borrell Fellowship program, and G. Fuster is supported by the Juan de la Cierva program.

The costs of publication of this article were defrayed in part by the payment of page charges. This article must therefore be hereby marked *advertisement* in accordance with 18 U.S.C. Section 1734 solely to indicate this fact.

Received February 26, 2019; revised September 15, 2019; accepted November 4, 2019; published first November 7, 2019.

References

1. Zubeldia-Plazaola A, Ametller E, Mancino M, Prats de Puig M, López-Plana A, Guzman F, et al. Comparison of methods for the isolation of human breast epithelial and myoepithelial cells. Front Cell Dev Biol 2015;3:32.
2. Perou CM, Jeffrey SS, van de Rijn M, Rees CA, Eisen MB, Ross DT, et al. Distinctive gene expression patterns in human mammary epithelial cells and breast cancers. Proc Natl Acad Sci U S A 1999;96:9212–7.
3. Perou CM, Sørlie T, Eisen MB, van de Rijn M, Jeffrey SS, Rees CA, et al. Molecular portraits of human breast tumours. Nature 2000;406:747–52.
4. Sorlie T, Perou CM, Tibshirani R, Aas T, Geisler S, Johnsen H, et al. Gene expression patterns of breast carcinomas distinguish tumor subclasses with clinical implications. Proc Natl Acad Sci U S A 2001;98:10869–74.
5. Carr JA, Havstad S, Zarbo RJ, Divine G, Mackowiak P, Velanovich V. The association of HER-2/neu amplification with breast cancer recurrence. Arch Surg 2000;135:1469–74.
6. Campone M, Berton-Rigaud D, Bourbouloux E, Sophie S, Zanetti A, Frenel JS. Her2 positive breast cancer: practices. Bulletin du cancer 2011;98:154–63.
7. Pinto AC, Ades F, de Azambuja E, Piccart-Gebhart M. Trastuzumab for patients with HER2 positive breast cancer: delivery, duration and combination therapies. Breast 2013;22:S152–5.
8. Baselga J, Swain SM. Novel anticancer targets: revisiting ERBB2 and discovering ERBB3. Nat Rev Cancer 2009;9:463–75.
9. Gomez HL, Doval DC, Chavez MA, Ang PC, Aziz Z, Nag S, et al. Efficacy and safety of lapatinib as first-line therapy for ErbB2-amplified locally advanced or metastatic breast cancer. J Clin Oncol 2008;26:2999–3005.
10. Dittmer J, Leyh B. The impact of tumor stroma on drug response in breast cancer. Semin Cancer Biol 2015;31:3–15.
11. Finak G, Bertos N, Pepin F, Sadekova S, Souleimanova M, Zhao H, et al. Stromal gene expression predicts clinical outcome in breast cancer. Nat Med 2008;14:518–27.
12. Werb Z, Lu P. The role of stroma in tumor development. Cancer J 2015;21:250–3.
13. Bhowmick NA, Neilson EG, Moses HL. Stromal fibroblasts in cancer initiation and progression. Nature 2004;432:332–7.
14. Orimo A, Weinberg RA. Stromal fibroblasts in cancer: a novel tumor-promoting cell type. Cell Cycle 2006;5:1597–601.
15. Kalluri R, Zeisberg M. Fibroblasts in cancer. Nat Rev Cancer 2006;6:392–401.
16. Karagiannis GS, Poutahidis T, Erdman SE, Kirsch R, Riddell RH, Diamandis EP. Cancer-associated fibroblasts drive the progression of metastasis through both paracrine and mechanical pressure on cancer tissue. Mol Cancer Res 2012;10:1403–18.
17. Luo H, Tu G, Liu Z, Liu M. Cancer-associated fibroblasts: a multifaceted driver of breast cancer progression. Cancer Lett 2015;361:155–63.
18. Howell A, Landberg G, Bergh J. Breast tumour stroma is a prognostic indicator and target for therapy. Breast Cancer Res 2009;11:S16.
19. Shiga K, Hara M, Nagasaki T, Sato T, Takahashi H, Takeyama H. Cancer-associated fibroblasts: their characteristics and their roles in tumor growth. Cancers 2015;7:2443–58.
20. Kerbel R, Folkman J. Clinical translation of angiogenesis inhibitors. Nat Rev Cancer 2002;2:727–39.
21. Majewski IJ, Nuciforo P, Mittempergher L, Bosma AJ, Eidtmann H, Holmes E, et al. PIK3CA mutations are associated with decreased benefit to neoadjuvant human epidermal growth factor receptor 2-targeted therapies in breast cancer. J Clin Oncol 2015;33:1334–9.
22. Nagy P, Friedländer E, Tanner M, Kapanen AI, Carraway KL, Isola J, et al. Decreased accessibility and lack of activation of ErbB2 in JIMT-1, a herceptin-resistant, MUC4-expressing breast cancer cell line. Cancer Res 2005;65:473–82.
23. Ma J, Lyu H, Huang J, Liu B. Targeting of erbB3 receptor to overcome resistance in cancer treatment. Mol Cancer 2014;13:105.
24. Nahta R, Yuan LX, Zhang B, Kobayashi R, Esteva FJ. Insulin-like growth factor-I receptor/human epidermal growth factor receptor 2 heterodimerization contributes to trastuzumab resistance of breast cancer cells. Cancer Res 2005;65:11118–28.
25. Kalluri R. The biology and function of fibroblasts in cancer. Nat Rev Cancer 2016;16:582–98.
26. Wheeler DL, Huang S, Kruser TJ, Nechrebecki MM, Armstrong EA, Benavente S, et al. Mechanisms of acquired resistance to cetuximab: role of HER (ErbB) family members. Oncogene 2008;27:3944–56.
27. Shattuck DL, Miller JK, Carraway KL 3rd, Sweeney C. Met receptor contributes to trastuzumab resistance of Her2-overexpressing breast cancer cells. Cancer Res 2008;68:1471–7.
28. Zhuang G, Brantley-Sieders DM, Vaught D, Yu J, Xie L, Wells S, et al. Elevation of receptor tyrosine kinase EphA2 mediates resistance to trastuzumab therapy. Cancer Res 2010;70:299–308.
29. Sanabria-Figueroa E, Donnelly SM, Foy KC, Buss MC, Castellino RC, Paplomata E, et al. Insulin-like growth factor-1 receptor signaling increases the invasive potential of human epidermal growth factor receptor 2-overexpressing breast cancer cells via Src-focal adhesion kinase and forkhead box protein M1. Mol Pharmacol 2015;87:150–61.
30. Falchook GS, Moulder SL, Wheler JJ, Jiang Y, Bastida CC, Kurzrock R. Dual HER2 inhibition in combination with anti-VEGF treatment is active in heavily pretreated HER2-positive breast cancer. Ann Oncol 2013;24:3004–11.
31. Garcia-Recio S, Pastor-Arroyo EM, Marín-Aguilera M, Almendro V, Gascón P. The transmodulation of HER2 and EGFR by Substance P in breast cancer cells requires c-Src and metalloproteinase activation. PLoS One 2015;10:e0129661.
32. Marusyk A, Tabassum DP, Janiszewska M, Place AE, Trinh A, Rozhok AI, et al. Spatial proximity to fibroblasts impacts molecular features and therapeutic sensitivity of breast cancer cells influencing clinical outcomes. Cancer Res 2016;76:6495–506.
33. Saito S, Morishima K, Ui T, Hoshino H, Matsubara D, Ishikawa S, et al. The role of HGF/MET and FGF/FGFR in fibroblast-derived growth stimulation and lapatinib-resistance of esophageal squamous cell carcinoma. BMC Cancer 2015;15:82.
34. Mao Y, Zhang Y, Qu Q, Zhao M, Lou Y, Liu J, et al. Cancer-associated fibroblasts induce trastuzumab resistance in HER2 positive breast cancer cells. Mol Biosyst 2015;11:1029–40.
35. Zazo S, González-Alonso P, Martín-Aparicio E, Chamizo C, Cristóbal I, Arpí O, et al. Generation, characterization, and maintenance of trastuzumab-resistant HER2+ breast cancer cell lines. Am J Cancer Res 2016;6:2661–78.
36. Mukohara T. Mechanisms of resistance to anti-human epidermal growth factor receptor 2 agents in breast cancer. Cancer Sci 2011;102:1–8.
37. Ye P, Zhang M, Fan S, Zhang T, Fu H, Su X,et al. Intra-Tumoral heterogeneity of HER2, FGFR2, cMET and ATM in gastric cancer: optimizing personalized healthcare through innovative pathological and statistical analysis. Plos One 2015;10:e0143207.
38. Yu Y, Yu X, Liu H, Song Q, Yang Y. miR494 inhibits cancerinitiating cell phenotypes and reverses resistance to lapatinib by downregulating FGFR2 in HER2positive gastric cancer. Int J Mol Med 2018;42:998–1007.
39. Liu YJ, Shen D, Yin X, Gavine P, Zhang T, Su X, et al. HER2, MET and FGFR2 oncogenic driver alterations define distinct molecular segments for targeted therapies in gastric carcinoma. Br J Cancer 2014;110:1169.
40. Nagatsuma AK, Aizawa M, Kuwata T, Doi T, Ohtsu A, Fujii H, et al. Expression profiles of HER2, EGFR, MET and FGFR2 in a large cohort of patients with gastric adenocarcinoma. Gastric Cancer 2015;18:227–38.
41. Wei W, Liu W, Serra S, Asa SL, Ezzat S. The breast cancer susceptibility FGFR2 provides an alternate mode of HER2 activation. Oncogene 2015 Feb 2. [Epub ahead of print].
42. Peiro G, Ortiz-Martínez F, Gallardo A, Pérez-Balaguer A, Sánchez-Payá J, Ponce JJ, et al. Src, a potential target for overcoming trastuzumab resistance in HER2-positive breast carcinoma. Br J Cancer 2014;111:689–95.
43. Tang CH, Yang RS, Chen YF, Fu WM. Basic fibroblast growth factor stimulates fibronectin expression through phospholipase C gamma, protein kinase C alpha, c-Src, NF-kappaB, and p300 pathway in osteoblasts. J Cell Physiol 2007;211:45–55.
44. Li X, Brunton VG, Burgar HR, Wheldon LM, Heath JK. FRS2-dependent SRC activation is required for fibroblast growth factor receptor-induced phosphorylation of Sprouty and suppression of ERK activity. J Cell Sci 2004;117:6007–17.
45. Acevedo VD, Ittmann M, Spencer DM. Paths of FGFR-driven tumorigenesis. Cell Cycle 2009;8:580–8.
46. Azuma K, Tsurutani J, Sakai K, Kaneda H, Fujisaka Y, Takeda M, et al. Switching addictions between HER2 and FGFR2 in HER2-positive breast tumor cells: FGFR2 as a potential target for salvage after lapatinib failure. Biochem Biophys Res Commun 2011;407:219–24.
47. Hanker AB, Garrett JT, Estrada MV, Moore PD, Ericsson PG, Koch JP, et al. HER2-overexpressing breast cancers amplify FGFR signaling upon acquisition of resistance to dual therapeutic blockade of HER2. Clin Cancer Res 2017;23:4323–34.
48. Piro G, Carbone C, Cataldo I, Di Nicolantonio F, Giacopuzzi S, Aprile G, et al. An FGFR3 autocrine loop sustains acquired resistance to trastuzumab in gastric cancer patients. Clin Cancer Res 2016;22:6164–75.